

Supporting Information

© Wiley-VCH 2011

69451 Weinheim, Germany

**Trinucleating Copper: Synthesis and Magnetostructural
Characterization of Complexes Supported by a Hexapyridyl
1,3,5-Triarylbenzene Ligand****

*Emily Y. Tsui, Michael W. Day, and Theodor Agapie**

anie_201005232_sm_miscellaneous_information.pdf

Supporting Information

Experimental Details

General Considerations	S2
Synthetic Procedures	S2
Figures S1–S9. ^1H and ^{13}C NMR spectra of H₃L , 1 , 2 , and 3	S8
Figures S10, S11. Variable Temperature ^1H NMR spectra of H₃L	S12
Figures S12, S13. 2D NMR spectra of H₃L	S13
Figure S14. Expanded ^1H NMR	S15
Table S1. Signal assignments and relaxation times of ^1H NMR spectrum of 2•3OTf	S15
Figure S15. 2D NMR spectra of 2•3OTf	S16
Figure S16. ^1H NMR spectra of the oxidation of 1•3OTf	S17
Figure S17–S19. ^1H NMR spectra of the titration of 2•3OTf with <i>n</i> Bu ₄ NBr and <i>n</i> Bu ₄ NI	S17

Magnetic Susceptibility Measurements

General Considerations	S19
Table S2. Magnetic Parameters for Fits Including θ	S19
Table S3. Magnetic Parameters for Fits Without θ	S19
Figures S20, S21. Plots of Magnetism Data for 2 , 3 With Fits (Including θ)	S20
Figures S22, S23. Plots of Magnetism Data for 2 , 3 With Fits (Without θ)	S21

Magnetostructural Study

Table S4. Structural and magnetic parameters for copper(II) trimers	S22
Figure S24. Plot of <i>J</i> vs. Cu–O–Cu bridge angle	S23

EPR Measurements

General Considerations	S24
Figures S24–28	S24

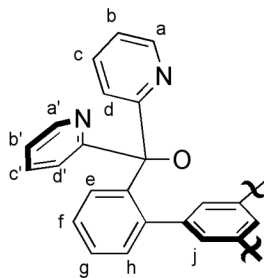
References	S27
-------------------	-----

Experimental Details

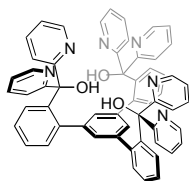
General Considerations. Unless stated otherwise, all synthetic manipulations were carried out using standard Schlenk techniques under a nitrogen atmosphere, or in a M. Braun glovebox under an atmosphere of nitrogen. Reactions were carried out in oven-dried glassware cooled under vacuum. Anhydrous THF was purchased from Aldrich in 18 L Pure-Pac™ containers. Anhydrous dichloromethane, acetonitrile, diethyl ether, and THF were purified by sparging with nitrogen for 15 minutes and then passing under nitrogen pressure through a column of activated A2 alumina (Zapp's). All non-dried solvents used were reagent grade or better. All NMR solvents were purchased from Cambridge Isotope Laboratories, Inc. NMR solvents were dried as follows: CD₂Cl₂ and CD₃CN over calcium hydride, and *d*₆-acetone over calcium sulfate. All NMR solvents were degassed by three freeze-pump-thaw cycles and vacuum-transferred prior to use. ¹H NMR and ¹³C NMR spectra were recorded on a Varian 300 MHz instrument or a Varian 500 MHz instrument or a Varian 600 MHz instrument, with shifts reported relative to the residual solvent peak. ¹⁹F NMR spectra were referenced to an external standard of CFC₃ (0 ppm). Elemental analyses were performed by Midwest Microlab, LLC, Indianapolis, IN. High resolution mass spectra (HRMS) were obtained at the California Institute of Technology Mass Spectral Facility. UV-Vis spectra were taken on a Varian Cary 50 spectrophotometer using a quartz crystal cell. IR spectra were recorded on a Nicolet 6700 FT-IR spectrometer using a solution cell with CaF₂ plates.

Unless indicated otherwise, all commercial chemicals were used as received. Copper(II) hydroxide phosphate, benzoin, and lithium bis(trimethylsilyl)amide was purchased from Aldrich. Di(2-pyridyl)ketone was purchased from Aldrich or from Frontier Chemicals. Copper(II) triflate and copper(II) tetrafluoroborate hydrate were purchased from Strem. Copper(I) triflate toluene dimer,^[1] tetrakis(acetonitrile)copper(I) perchlorate,^[2] and 1,3,5-tris(2-bromophenyl)benzene^[3] were prepared according to literature procedures.

For ¹H NMR spectra discussed below, refer to Scheme 1 for signal assignments. In some of the compounds, the protons of the two pyridine moieties are related by symmetry and protons assigned as (a, b, c, d) will refer to protons (a', b', c', d') as well.

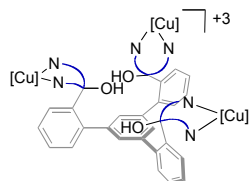


Scheme 1. Proton assignments for complexes of **H₃L**.



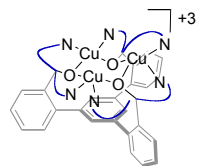
Synthesis of 1, 3, 5-Tris(2-di(2'-pyridyl)hydroxymethylphenyl)benzene (H₃L). In the glovebox, a Schlenk flask equipped with a stir bar was charged with 1,3,5-tris(2-bromophenyl)benzene (4.0 g, 7.37 mmol) and diethyl ether (80 mL). On the Schlenk line, the suspension was cooled to -78 °C, and *t*-BuLi (1.61 M, 27.9 mL, 44.9 mmol) was added slowly via syringe. The mixture was stirred for 15 min. at -78 °C, and a solution of di(2-pyridyl)ketone (4.21 g, 22.8 mmol) in diethyl ether (30 mL) was added slowly

via cannula transfer. The reaction mixture was allowed to warm to room temperature and stirred for 8 h under nitrogen. The mixture was quenched with methanol (30 mL), and the orange solution was diluted with water and extracted with dichloromethane. The organic layer was washed with brine and dried over magnesium sulfate, then filtered. The solvent was removed under reduced pressure, and the yellow residue was recrystallized from acetone/dichloromethane to yield the product as a white solid (2.65 g, 42%). ^1H NMR (300 MHz, CDCl_3 , 25 °C): δ 8.41 (d, $J = 6$ Hz, 6 H, *a*), 7.66 (bs, 6 H, *c*), 7.55 (bs, 6 H, *d*), 7.25 (t, $J = 7.5$ Hz, 3 H, *f*), 7.13 (t, $J = 7.5$ Hz, 3 H, *g*), 7.02 (bs, 6 H, *b*), 6.81 (bs, 3 H, *e*), 6.74 ($J = 6$ Hz, 3 H, *h*), 6.37 (bs, 3 H, OH), 6.14 (bs, 3 H, *j*). ^{13}C NMR (CDCl_3): δ 164.0, 147.2, 144.0, 143.5, 139.5, 136.2, 133.2, 129.2, 126.6, 126.1, 123.7, 121.9, 81.9. IR (CH_2Cl_2): 3330, 1751 cm^{-1} . HRMS (FAB⁺): calcd. for $\text{C}_{57}\text{H}_{43}\text{N}_6\text{O}_3$: 859.3397; found: 859.3436 [M+H].



Synthesis of $[(\text{H}_3\text{L})\text{Cu}_3](3\text{OTf})$ (1•3OTf**).** In the glovebox, a 20-mL scintillation vial equipped with a stir bar was charged with a suspension of **H₃L** (0.100 g, 0.116 mmol) in acetonitrile (10 mL). A solution of $[\text{CuOTf}]_2 \cdot \text{toluene}$ (0.090 g, 0.175 mmol) in acetonitrile (5 mL) was added slowly. The resulting yellow solution was stirred for 15 min. at room temperature, and the solvent was removed under reduced pressure to yield a yellow-orange solid (172 mg, 85%). ^1H NMR (300 MHz, CD_3CN): δ 8.32 (bs, 6 H, *a*), 7.81 (bs, 12 H, *c* & *d*), 7.45 (t, $J = 7.5$ Hz, 3 H, *f*), 7.23 (m, 6 H, *g*), 7.23 (bs, 3 H, *b*), 6.87 (bs, 3 H, *e*), 6.74 (bs, 3 H, *h*), 6.22 (bs, 3 H, OH), 5.23 (bs, 3 H, *j*). ^{13}C NMR (125.7 MHz, CD_3CN): δ 163.7, 149.5, 144.1, 142.8, 138.9, 135.1, 131.7, 129.8, 129.1, 127.9, 124.4, 123.8, 121.3, 82.9. ^{19}F NMR (282.3 MHz, CD_2Cl_2): δ 78.97. IR (CH_2Cl_2): 3337, 1600 cm^{-1} . UV-vis (CH_3CN , λ_{max} (ϵ)): 260 (35,500 $\text{M}^{-1} \text{cm}^{-1}$); 381 (610 $\text{M}^{-1} \text{cm}^{-1}$) nm. Anal. Calcd. for $\text{C}_{72}\text{H}_{60}\text{Cu}_3\text{F}_9\text{N}_{12}\text{O}_{12}\text{S}_3$ (6 CH_3CN): C, 49.61; H, 3.47; N, 9.64. Anal. Calcd. for $\text{C}_{66}\text{H}_{51}\text{Cu}_3\text{F}_9\text{N}_9\text{O}_{12}\text{S}_3$ (3 CH_3CN): C, 48.93; H, 3.17; N, 7.78. Found: C, 47.25; H, 3.16; N, 7.52.

Synthesis of $[(\text{H}_3\text{L})\text{Cu}_3](3\text{ClO}_4)$ (1•3ClO₄**).** In the glovebox, a 20-mL scintillation vial equipped with a stir bar was charged with a suspension of **H₃L** (0.050 g, 0.058 mmol) in acetonitrile (5 mL). While stirring, a solution of tetrakis(acetonitrile) copper(I) perchlorate (0.057 g, 0.175 mmol) in acetonitrile (5 mL) was added, and the yellow solution was stirred at room temperature for 5 h. The reaction mixture was concentrated under vacuum to a volume of 5 mL, and a yellow solid was then precipitated out upon addition of diethyl ether (10 mL). The yellow solid was collected and washed with diethyl ether, then extracted with dichloromethane (10 mL). The solvent was removed under reduced pressure from the yellow dichloromethane extract to yield the product as a yellow solid (57 mg, 61%). ^1H NMR spectra in CD_3CN and CD_2Cl_2 match that of **1•3OTf**. IR (CH_2Cl_2): 3393, 1599, 1103 cm^{-1} . UV-vis (CH_3CN , λ_{max} (ϵ)): 262 (42,000 $\text{M}^{-1} \text{cm}^{-1}$); 378 (670 $\text{M}^{-1} \text{cm}^{-1}$) nm. Anal. Calcd. for $\text{C}_{69}\text{H}_{60}\text{Cl}_3\text{Cu}_3\text{N}_{12}\text{O}_{15}$: C, 51.98; H, 3.79; N, 10.54. Found: C, 51.37; H, 3.69; N, 10.30.



Synthesis of $[(\text{L})\text{Cu}_3](3\text{OTf})$ (2•3OTf**).**

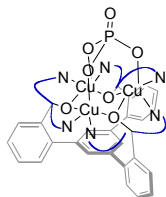
Method A: In the glovebox, a 20-mL scintillation vial equipped with a stir bar was charged with a solution of **H₃L** (0.500 g, 0.582 mmol) in THF (8 mL). The solution was frozen in a cold well. While stirring, a solution of LiHMDS (0.292 g, 1.75 mmol) in THF was added slowly to the thawing solution.

The yellow solution was stirred at room temperature for 15 min., then frozen again. A suspension of copper(II) trifluoromethanesulfonate (0.632 g, 1.75 mmol) in 1:1 THF/CH₃CN (4 mL) was added to the thawing solution, and the green suspension was stirred at room temperature for 1 h. The green precipitate was collected on a fritted glass funnel over Celite, and washed with THF, then extracted with acetonitrile. The solution was concentrated under reduced pressure to yield the product as a blue-green solid (0.604 g, 70%). The product can be recrystallized from CH₃CN/THF to yield hexagonal blue green crystals (0.110 g, 13%). ¹H NMR (600 MHz, CD₃CN): δ 126.72 (bs, 3 H, *a/a'*), 104.99 (bs, 3 H, *a/a'*), 51.44 (s, 3 H, *b*), 45.43 (s, 3 H, *b'*), 36.53 (s, 3 H, *d'*), 30.42 (s, 3 H, *d*), 13.34 (s, 3 H, *c*), 11.81 (s, 3 H, *c'*), 11.61 (bs, 3 H, *j*), 9.46 (s, 3 H, *f*), 9.08 (s, 3 H, *h*), 6.96 (s, 3 H, *e*), 6.91 (s, 3 H, *g*). ¹⁹F NMR (282 MHz, CD₃CN): δ -78.77. UV-Vis (CH₃CN, λ_{max} (ε)): 253 (63,600 M⁻¹ cm⁻¹); 681 (330 M⁻¹ cm⁻¹) nm. HRMS (FAB+): calcd. for C₅₇H₃₉Cu₃N₆O₃ (no ⁻OTf): 1046.0965; found: 1046.0985 [M⁺]; 1195.0427 [M•1OTf]; 1343.9903 [M•2OTf]. Anal. Calcd. for C₆₀H₃₉Cu₃F₉N₆O₁₂S₃: C, 48.24; H, 2.63; N, 5.63. Found: C, 47.91; H, 2.90; N, 5.76.

Method B: In the glovebox, a J Young NMR tube was charged with **1•3OTf** (16.9 mg, 0.01 mmol) in 0.7 mL CD₃CN. On a Schlenk line, the solution was degassed with one freeze-pump-thaw cycle. The solution was frozen again, and the tube was evacuated and put under an atmosphere of O₂. The solution was then allowed to warm up to room temperature. The yellow solution turned green and then darker blue-green over the course of 12 h. The ¹H NMR spectrum matches that of **2•3OTf** prepared in the way described above.

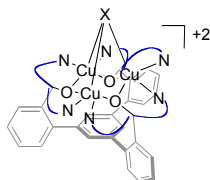
The ¹H NMR spectra of the other derivatives of compounds **2** and **3** have not been assigned, but are similar to that of **2•3OTf**.

Synthesis of [(L)Cu₃](BF₄)₃ (2•3BF₄**).** Under ambient conditions, a scintillation vial equipped with a stir bar was charged with **H₃L** (0.200 g, 0.233 mmol) and Cu(BF₄)₂•XH₂O (0.193 g, ca. 0.815 mmol). The mixture was suspended in acetonitrile (5 mL), and triethylamine (0.16 mL, 1.16 mmol) was added via syringe. The blue-green mixture was stirred at room temperature for 10 h, and the solvent was removed *in vacuo*. The blue-green residue was washed with THF, then extracted with acetonitrile. The solution was concentrated *in vacuo*, then recrystallized from CH₃CN/Et₂O to yield the product as blue-green crystals of **2•3BF₄•Et₂O** (0.043 g, 13%). ¹H NMR (300 MHz, CD₃CN): δ 125.66 (bs, 3 H), 100.08 (bs, 3 H), 49.31 (s, 3 H), 46.62 (s, 3 H), 37.46 (s, 3 H), 28.93 (s, 3 H), 13.18 (s, 3 H), 11.72 (s, 3 H), 11.30 (s, 3 H), 9.69 (s, 3 H), 9.12 (s, 3 H), 6.85 (s, 3 H), 6.64 (s, 3 H). ¹⁹F NMR (282.3 MHz, CD₃CN): δ -149.25. UV-Vis (CH₃CN, λ_{max} (ε)): 246 (53,300 M⁻¹ cm⁻¹), 730 (336 M⁻¹ cm⁻¹) nm. Anal. Calcd. for C₅₇H₃₉B₃Cu₃F₁₂N₆O₃: C, 52.39; H, 3.01; N, 6.43. Calcd. for C₆₁H₄₉B₃Cu₃F₁₂N₆O₄ (**2•3BF₄•Et₂O**): C, 53.05; H, 3.58; N, 6.08. Found: C, 53.29; H, 3.68; N, 6.13.



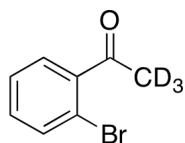
Synthesis of [(L)Cu₃](PO₄) (2•PO₄**).** Under ambient conditions, a scintillation vial equipped with a stir bar was charged with **H₃L** (0.200 g, 0.233 mmol) and Cu₂(OH)PO₄ (0.084 g, 0.349 mmol). The mixture was suspended in 2:1 H₂O/acetone (15 mL), and phosphoric acid (85%, 0.016 mL) was added via syringe. The green mixture was stirred for 1 day, then filtered through Celite. The solvent was removed from the green filtrate *in vacuo* to yield the product as a green solid (0.210 g, 79%). ¹H NMR (300 MHz, D₂O): δ 148.94 (bs, 3 H), 101.47 (bs, 3 H), 56.33 (s, 3 H), 50.50 (s, 3 H), 39.66 (s, 3 H), 29.70 (s, 3 H), 13.44 (s, 3 H), 11.19 (bs, 3 H), 10.81 (s, 3 H), 10.21 (s, 3 H), 9.58 (s, 3 H), 6.64 (s, 3 H), 5.76 (s, 3 H). UV-Vis (H₂O, λ_{max} (ε)): 245 (28,500 M⁻¹ cm⁻¹), ~800 (260 M⁻¹ cm⁻¹) nm. Anal. Calcd. for C₅₇H₅₆Cu₃N₆O₁₈P₂

(**2**•**PO₄**•**H₃PO₄**•**6H₂O**): C, 50.80; H, 4.04, N, 6.24. Found: C, 49.91; H, 3.88; N, 6.00. An X-ray diffraction study of a single crystal of **2**•**PO₄** showed that the compound crystallizes with a disordered amount of H₂O and additional phosphate anions within the unit cell.

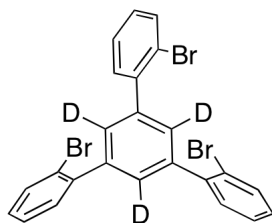


Synthesis of [(L)Cu₃]Br(OTf)₂ (3**•**Br**•**2OTf**).** Under ambient conditions, a scintillation vial equipped with a stir bar was charged with **2**•**3OTf** (0.056 g, 0.0372 mmol) in acetonitrile (6 mL). A solution of tetrabutylammonium bromide (0.012 g, 0.0372 mmol) in acetonitrile (2 mL) was added, and the green solution was stirred at room temperature for 3 h. The solvent was removed *in vacuo*, and the green residue was washed with THF, then extracted with acetonitrile. The solution was concentrated to yield the product as a green solid (0.047 g, 89 %). The compound crystallizes from vapor diffusion of THF into a CH₃CN solution of **3**•**Br**•**2OTf** with an additional equivalent of THF. ¹H NMR (300 MHz, CD₃CN): δ 154.39 (s, 3 H), 124.72 (s, 3 H), 61.15 (s, 3 H), 56.92 (s, 3 H), 41.73 (s, 3 H), 36.15 (s, 3 H), 14.33 (s, 3 H), 11.73 (s, 3 H), 11.47 (s, 3 H), 11.25 (s, 3 H), 9.38 (s, 3 H), 7.24 (s, 3 H), 6.36 (s, 3 H). ¹⁹F NMR (282.3 MHz, CD₃CN): δ -78.54. UV-Vis (CH₃CN, λ_{max} (ε)): 245 (75,000 M⁻¹ cm⁻¹), 725 (707 M⁻¹ cm⁻¹) nm. Anal. Calcd. for C₆₃H₄₆BrCu₃F₆N₆O₁₀S₂ (**3**•**Br**•**2OTf**•**THF**): C, 50.59; H, 3.10; N, 5.62. Found: C, 50.32; H, 3.32; N, 5.41.

Synthesis of [(L)Cu₃]I(OTf)₂ (3**•**I**•**2OTf**).** Under ambient conditions, a scintillation vial equipped with a stir bar was charged with **2**•**3OTf** (0.051 g, 0.034 mmol) in acetonitrile (6 mL). A solution of tetrabutylammonium iodide (0.012 g, 0.034 mmol) in acetonitrile (2 mL) was added, and the green solution was stirred at room temperature for 3 h. The solvent was removed *in vacuo*, and the green residue was washed with THF, then extracted with acetonitrile. The solution was concentrated to yield the product as a green solid that was recrystallized from CH₃CN/THF to yield hexagonal green crystals (0.032 g, 64 %). ¹H NMR (300 MHz, CD₃CN): δ 141.31 (s, 3 H), 116.58 (s, 3 H), 57.45 (s, 3 H), 53.43 (s, 3 H), 40.13 (s, 3 H), 34.07 (s, 3 H), 14.11 (s, 3 H), 11.57 (s, 3 H), 11.32 (s, 3 H), 10.86 (s, 3 H), 8.30 (s, 3 H), 7.10 (s, 3 H), 6.47 (s, 3 H). ¹⁹F NMR (282.3 MHz, CD₃CN): δ -78.60. UV-Vis (CH₃CN, λ_{max} (ε)): 246 (41,500 M⁻¹ cm⁻¹), 406 (shoulder, 805 M⁻¹ cm⁻¹), 709 (545 M⁻¹ cm⁻¹) nm. Anal. Calcd. for C₅₉H₃₉Cu₃F₆I₁N₆O₉S₂: C, 48.15; H, 2.67; N, 5.71. Found: C, 48.24; H, 2.70; N, 5.49.



D₃-2'-bromoacetophenone. A Schlenk flask equipped with a stir bar was charged with NaOH (0.03 g) and flame-dried under vacuum. D₂O (8 mL, 400 mmol) and 2'-bromoacetophenone (1.6 mL, 12 mmol) were added via syringe, and the mixture was stirred at room temperature under nitrogen for 40 h. Anhydrous diethyl ether (10 mL) was added, and the organics were extracted, dried over magnesium sulfate, and filtered. The solvent was removed under reduced pressure to yield the product as a colorless oil. ¹H NMR spectroscopy indicated 16% of the doubly deuterated compound. The product was carried on without further purification.



D₃-1,3,5-tris(2-bromophenyl)benzene. A flame-dried Schlenk flask equipped with a stir bar was charged with D₃-2'-bromoacetophenone and then fit with a Teflon stopper. The flask was evacuated for 5 min., then fit with a septum. Trifluoromethanesulfonic acid (0.05 mL) was added via syringe. The yellow-orange mixture was stirred at 130 °C for 14 h, then cooled to room temperature. The mixture was quenched with D₂O (2 mL) and CH₂Cl₂. The organics were extracted, dried over magnesium sulfate, and filtered. The solvent was removed *in vacuo*, and the red residue was taken up in CH₂Cl₂ (5 mL). The product precipitated out of solution was a white solid upon addition of methanol. The solid was collected on a fritted glass funnel and further washed with methanol, then dried under vacuum (0.896 g, 41%). ¹H NMR spectroscopy indicated 30% of the doubly-deuterated product.

D₃-H₃L. In a glove box, D₃-1,3,5-tris(2-bromophenyl)benzene (0.57 g, 1.05 mmol) was added to a scintillation vial equipped with a stir bar and then suspended in diethyl ether (10 mL). The mixture was frozen in a cold well. To the stirred, thawing mixture, *t*-BuLi (1.61 M in hexanes, 3.97 mL, 6.39 mmol) was added via syringe. The dark red mixture was stirred for 10 min. at room temperature, then frozen again. To the thawing red mixture was added a thawing solution of di(2-pyridyl)ketone in THF (4 mL). The mixture was allowed to warm to room temperature and stirred for 7 h, turning green and then brown. The vial was removed from the glovebox, and the reaction was quenched with water. The precipitated orange solid was collected on a fritted funnel and washed with H₂O and diethyl ether. The solid was dissolved in CH₂Cl₂, and the solution was washed with H₂O and brine. The organic layer was dried over magnesium sulfate and filtered, and the solvent was removed *in vacuo*. The residue was recrystallized from CH₂Cl₂/diethyl ether to yield the product as a white solid (0.108 g, 12%).

D₃-1•3OTf. In a glove box, D₃-H₃L (0.050 g, 0.058 mmol) and (CuOTf)₂•toluene (0.045 g, 0.087 mmol) were added to a scintillation vial equipped with a stir bar and dissolved in acetonitrile (5 mL). The orange solution was stirred at room temperature for 15 min. The solvent was removed under reduced pressure to yield the product as an orange-yellow solid (0.090 g, 88%).

Oxidation of 1•3OTf

1 equiv: In the glovebox, a scintillation vial equipped with a stir bar was charged with a solution of 1•3OTf (0.050 g, 0.0287 mmol) in acetonitrile (8 mL). A stock solution (0.020 mL Et₃N/5 mL CH₃CN) was prepared in a second vial, and 1 mL (1 equiv) was added to the yellow solution. A second stock solution (0.037 g AgOTf/5 mL CH₃CN) was prepared in a vial, and 1 mL (1 equiv) was added to the solution of 1•3OTf. The yellow mixture was stirred at room temperature for 12 h, during which the solution turned pale green and a silver mirror was formed. The mixture was filtered, and the green filtrate was concentrated *in vacuo* to a green solid. The ¹H NMR spectrum of a portion of the residue in CD₃CN corresponds to a 1:2 mixture of 2•3OTf and 1•3OTf (Figure S20).

2 equiv: The same mixture from before was redissolved in CH₃CN (8 mL), and 1 mL each of the stock solutions of Et₃N and AgOTf were added. The green mixture was stirred for another 12 h at room temperature, filtered, and concentrated. The ¹H NMR spectrum of a portion of the residue in CD₃CN corresponds to a 2:1 mixture of 2•3OTf and 1•3OTf.

3 equiv: The procedure above was repeated with an additional equivalent of Et₃N and AgOTf. The mixture was stirred for 12 h at room temperature, filtered, and concentrated. The ¹H NMR spectrum of a portion of the residue in CD₃CN shows complete conversion of 1•3OTf to 2•3OTf.

Reduction of 2

A Schlenk tube with a Teflon stopper and equipped with a stir bar was charged with **2•3OTf** (0.015 g, 0.01 mmol) and $\text{Et}_3\text{N}\cdot\text{HCl}$ (0.004 g, 0.03 mmol) in acetonitrile (5 mL). The green mixture was degassed with three freeze-pump-thaw cycles, then fitted with a septum under N_2 . A solution of CoCp_2 (0.005 g, 0.03) in THF (1.2 mL) was added, and the mixture turned yellow-brown. The solvent was removed from the mixture under reduced pressure. The ^1H NMR spectrum of the residue in CD_3CN matches that of **1•3OTf**.

NMR Spectra

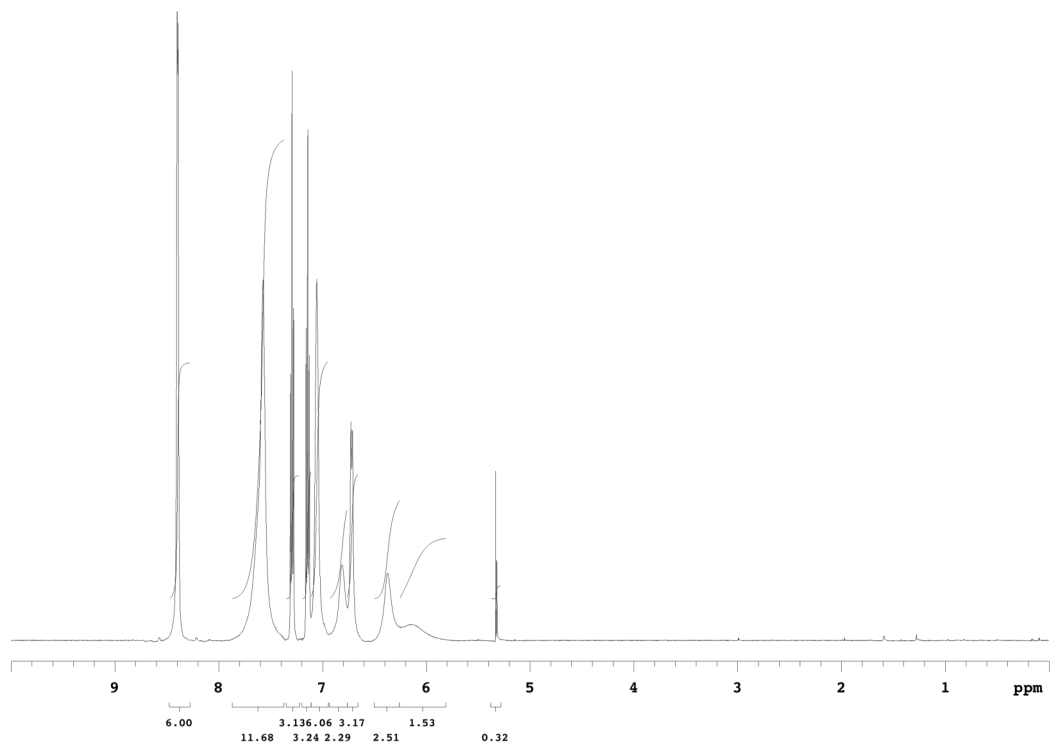


Figure S1. ^1H NMR spectrum of H_3L in CD_2Cl_2 at 25°C .

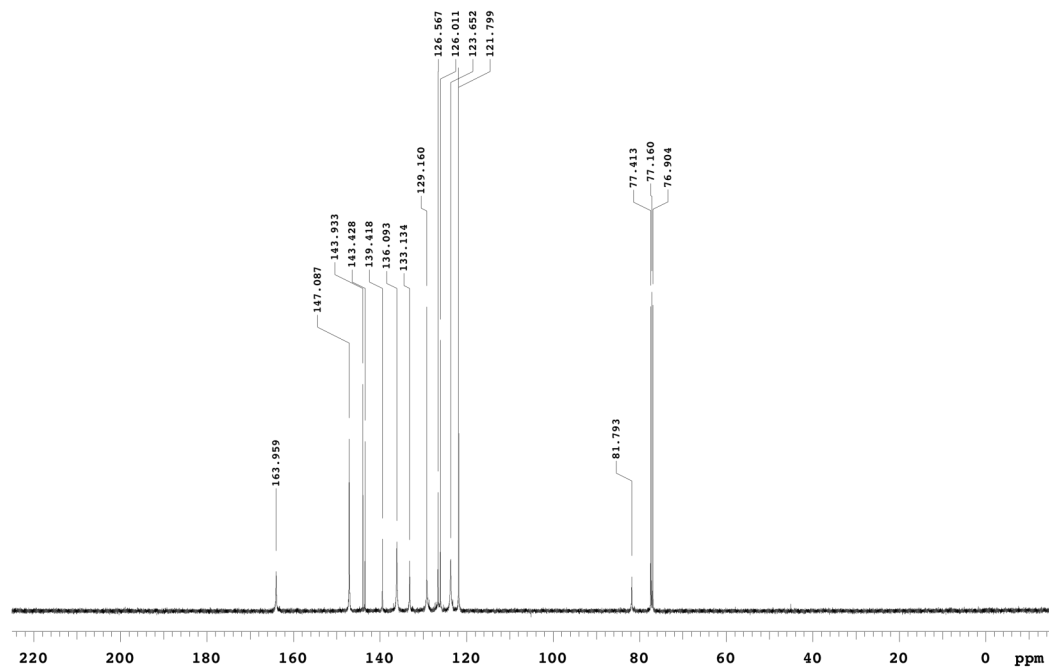


Figure S2. ^{13}C NMR spectrum of H_3L in CDCl_3 at 25°C .

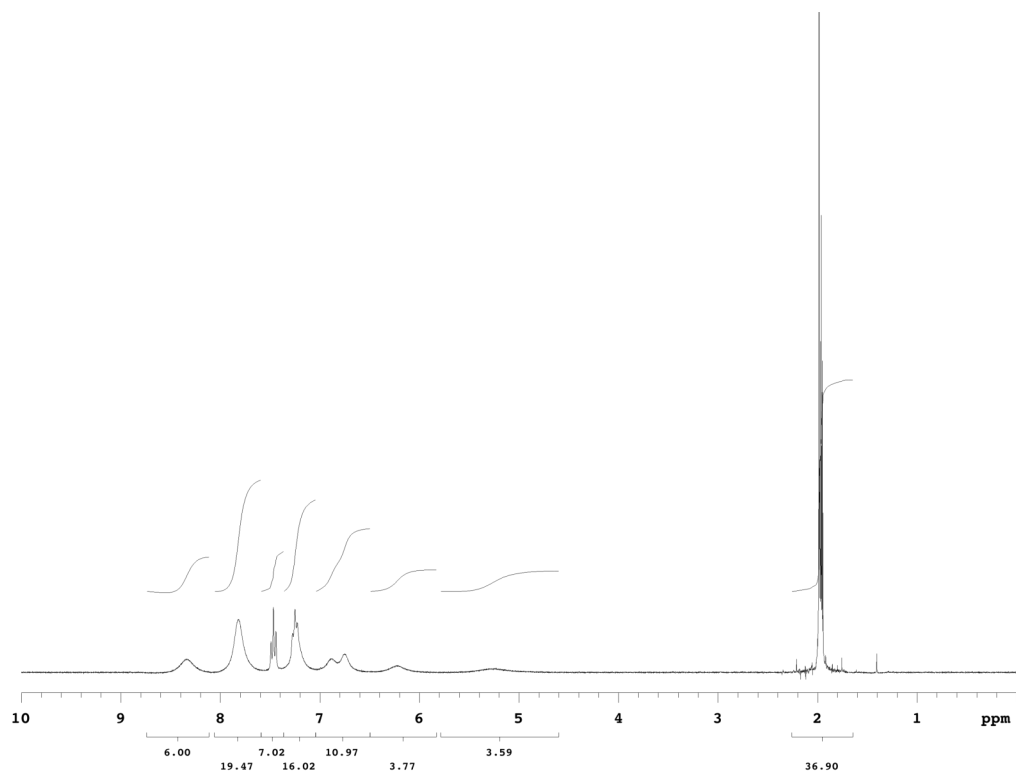


Figure S3. ^1H NMR spectrum of $1 \cdot 3\text{OTf}$ in CD_3CN at 25°C . CH_3CN peak is offscale.

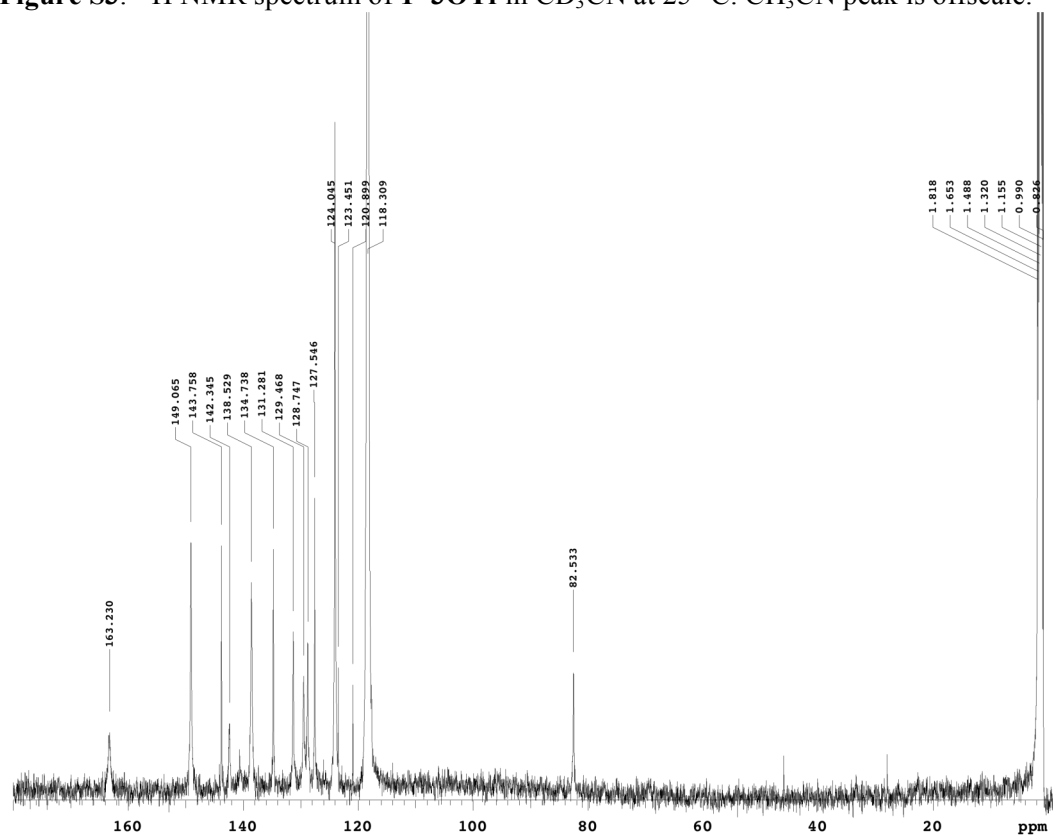


Figure S4. ^{13}C NMR spectrum of $1 \cdot 3\text{OTf}$ in CD_3CN at 25°C . CD_3CN residual peaks are offscale.

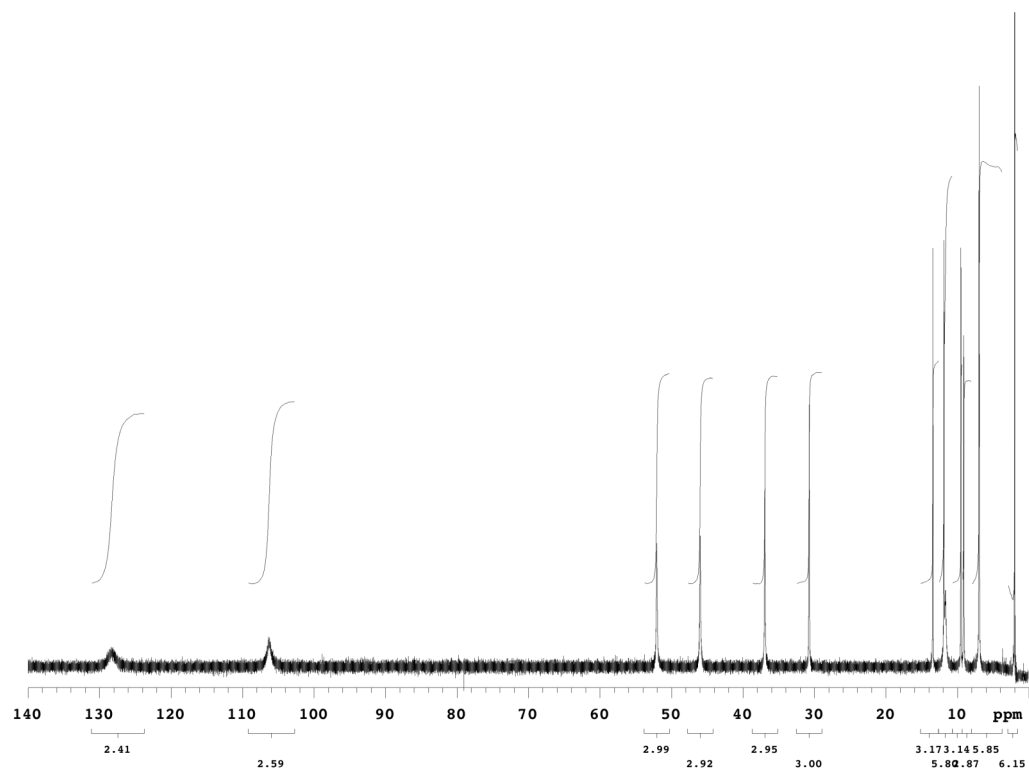


Figure S5. ^1H NMR spectrum of $2 \cdot 3\text{OTf}$ in CD_3CN at 25°C . CD_3CN solvent residual peak is offscale.

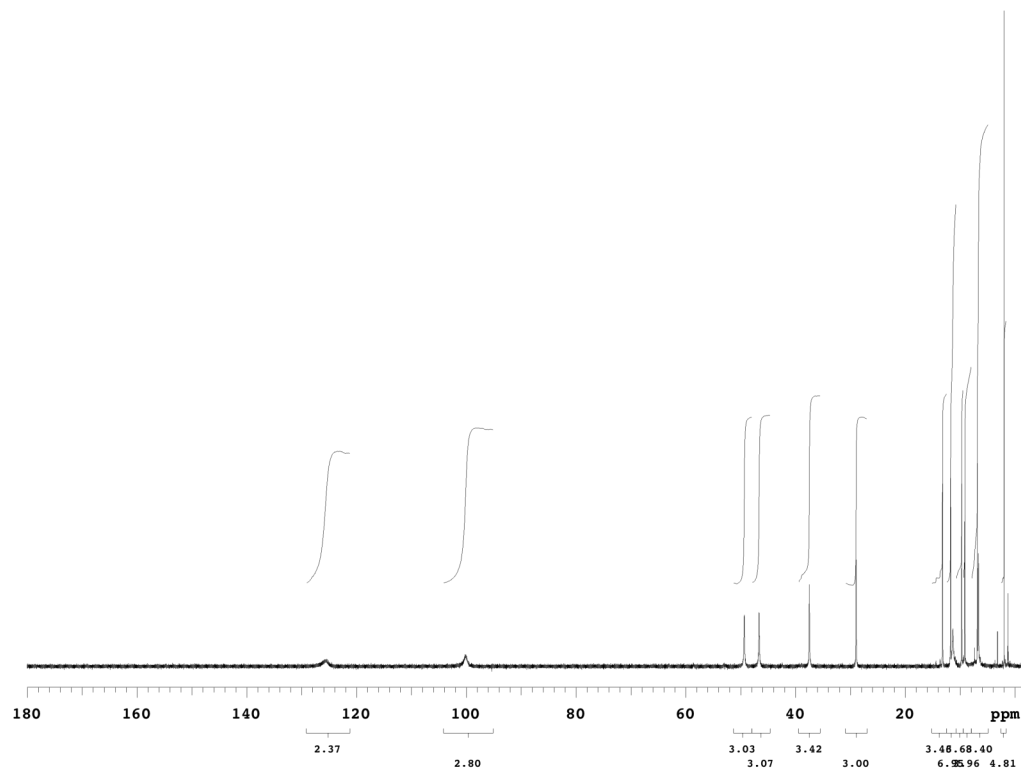


Figure S6. ^1H NMR spectrum of $2 \cdot 3\text{BF}_4$ in CD_3CN at 25°C .

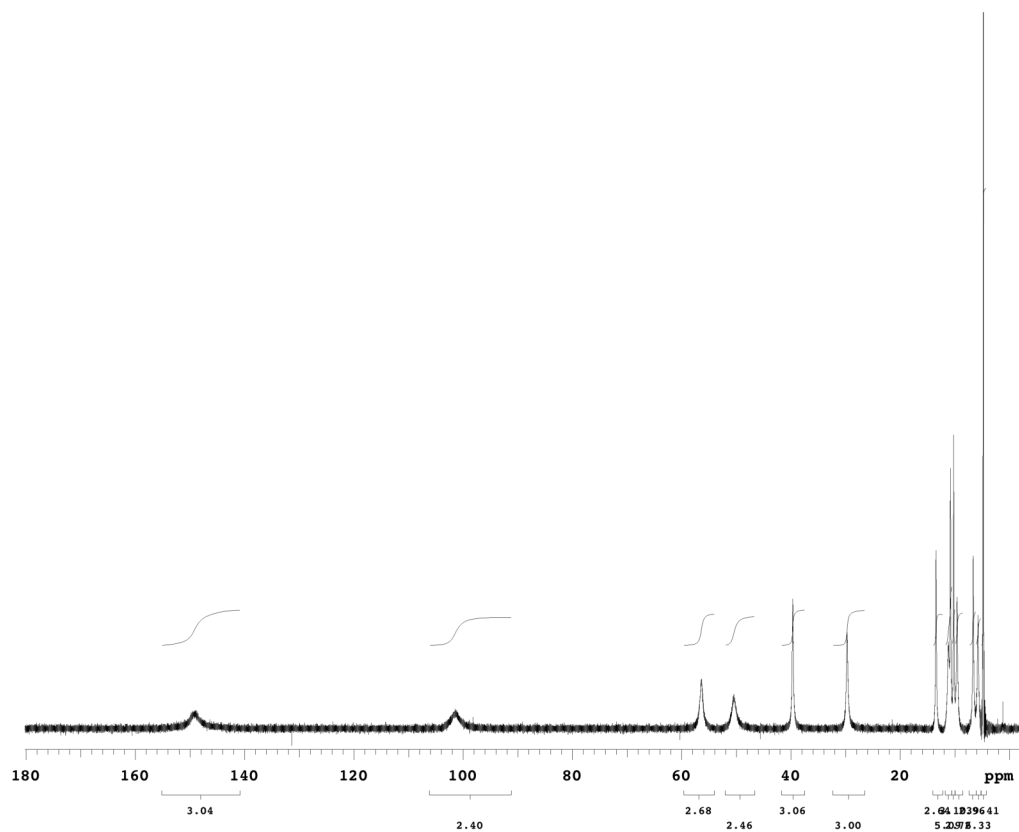


Figure S7. ^1H NMR spectrum of $2 \cdot \text{PO}_4$ in D_2O at $25\text{ }^\circ\text{C}$. D_2O solvent residual peak is offscale.

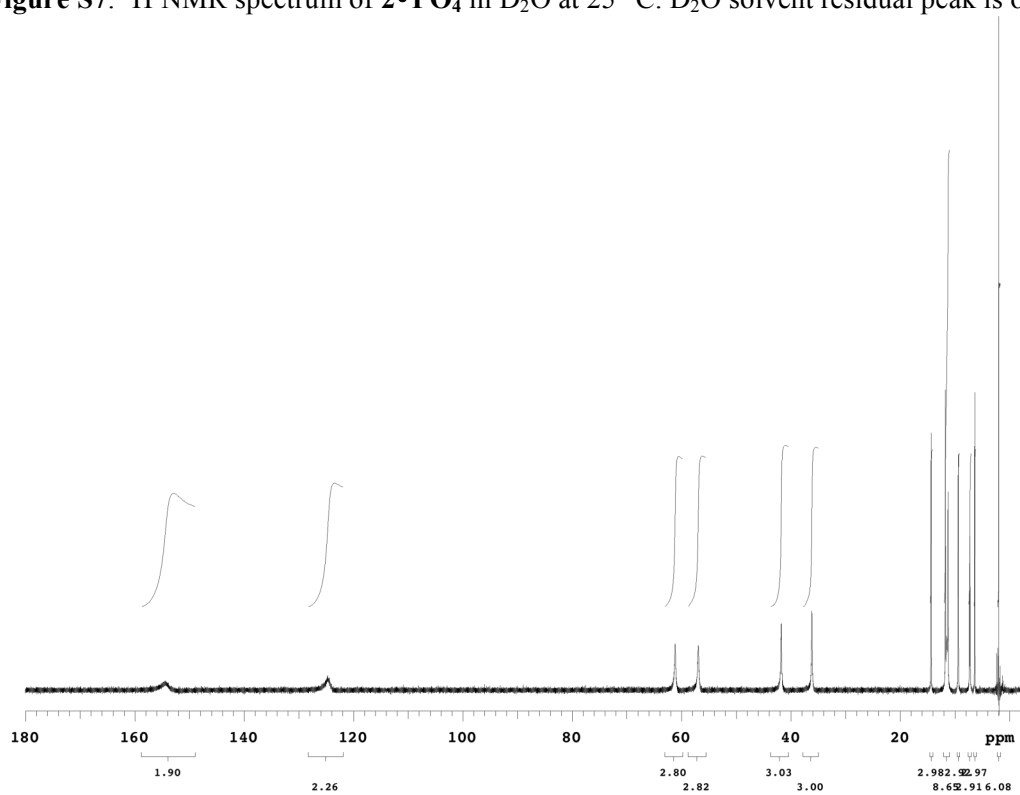


Figure S8. ^1H NMR spectrum of $3 \cdot \text{Br} \cdot 2\text{OTf}$ in CD_3CN at $25\text{ }^\circ\text{C}$. CD_3CN residual peak is offscale.

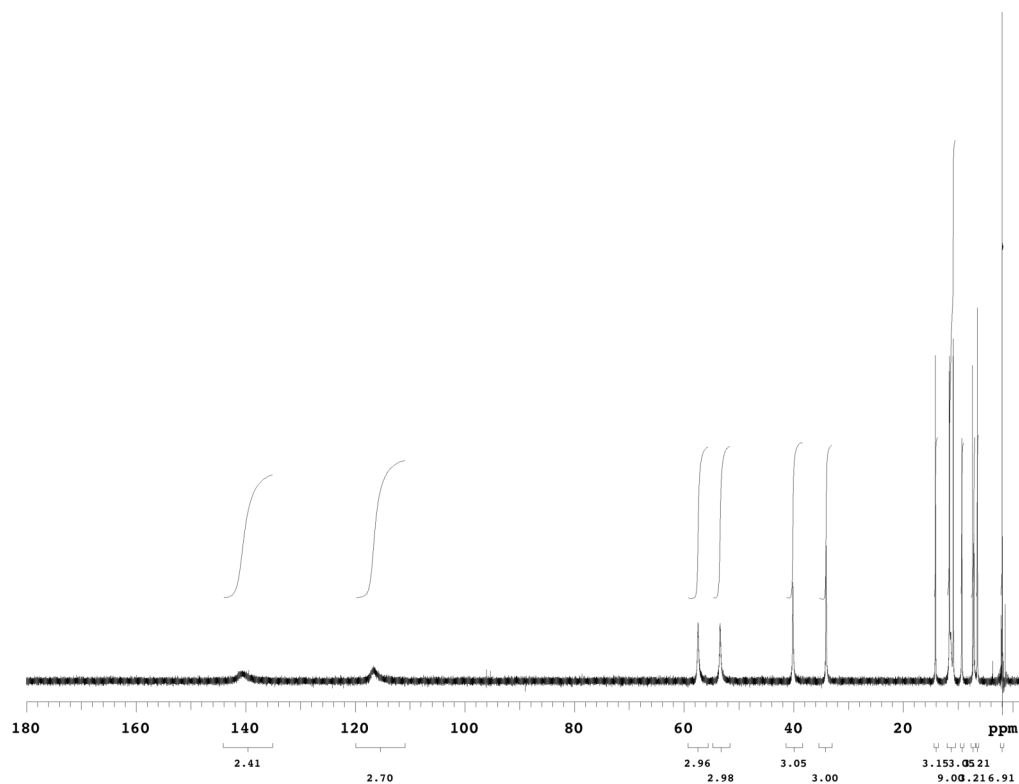


Figure S9. ¹H NMR spectrum of **3•I•2OTf** in CD₃CN at 25 °C. CD₃CN residual peak is offscale.

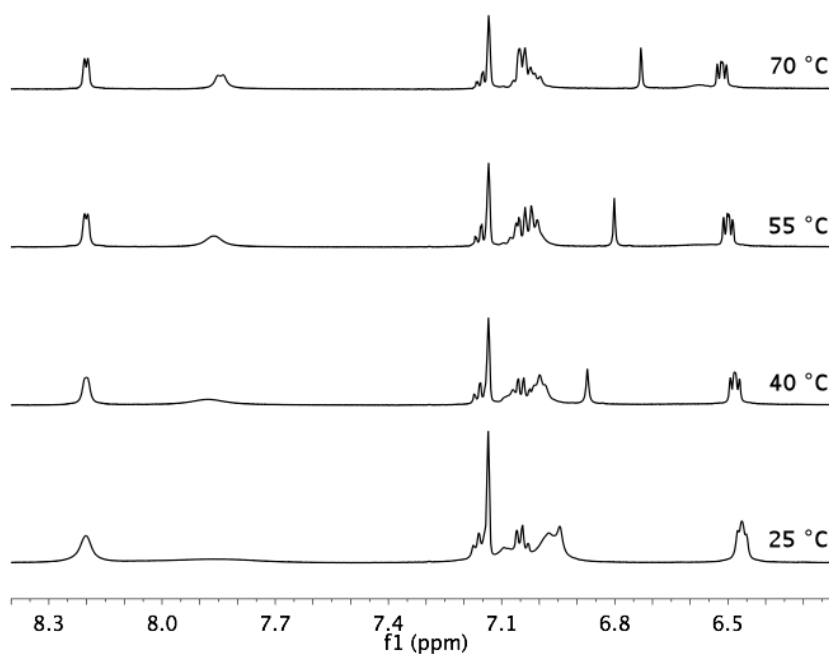


Figure S10. Variable temperature ¹H NMR spectra of **H₃L** in C₆D₆.

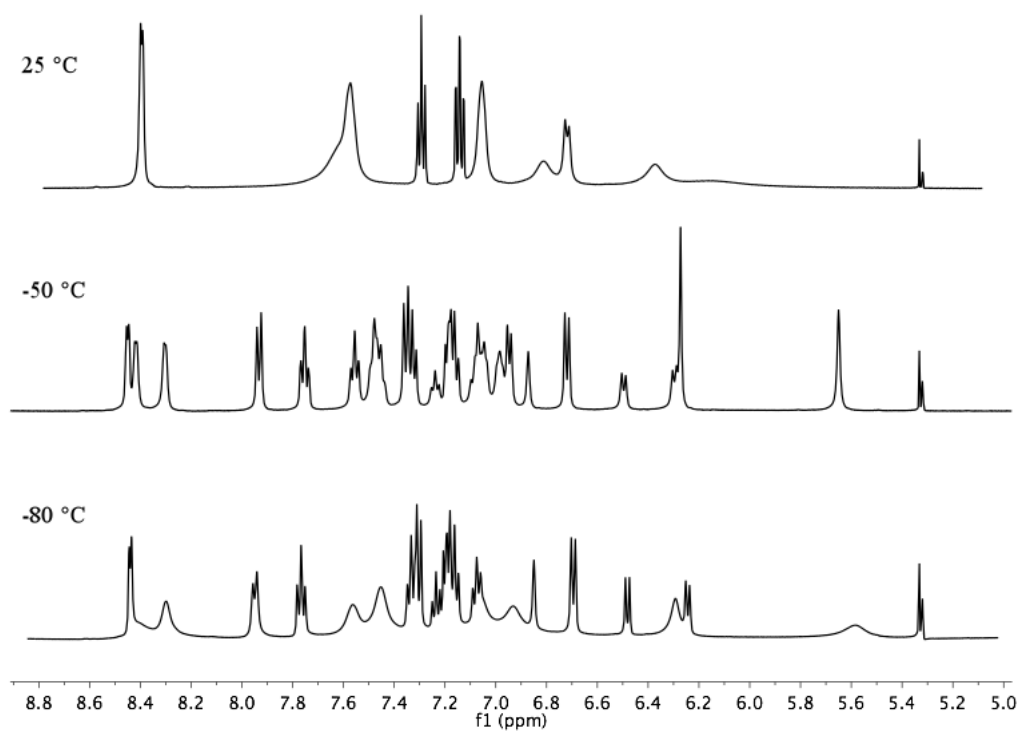


Figure S11. Variable temperature ^1H NMR spectra of H_3L

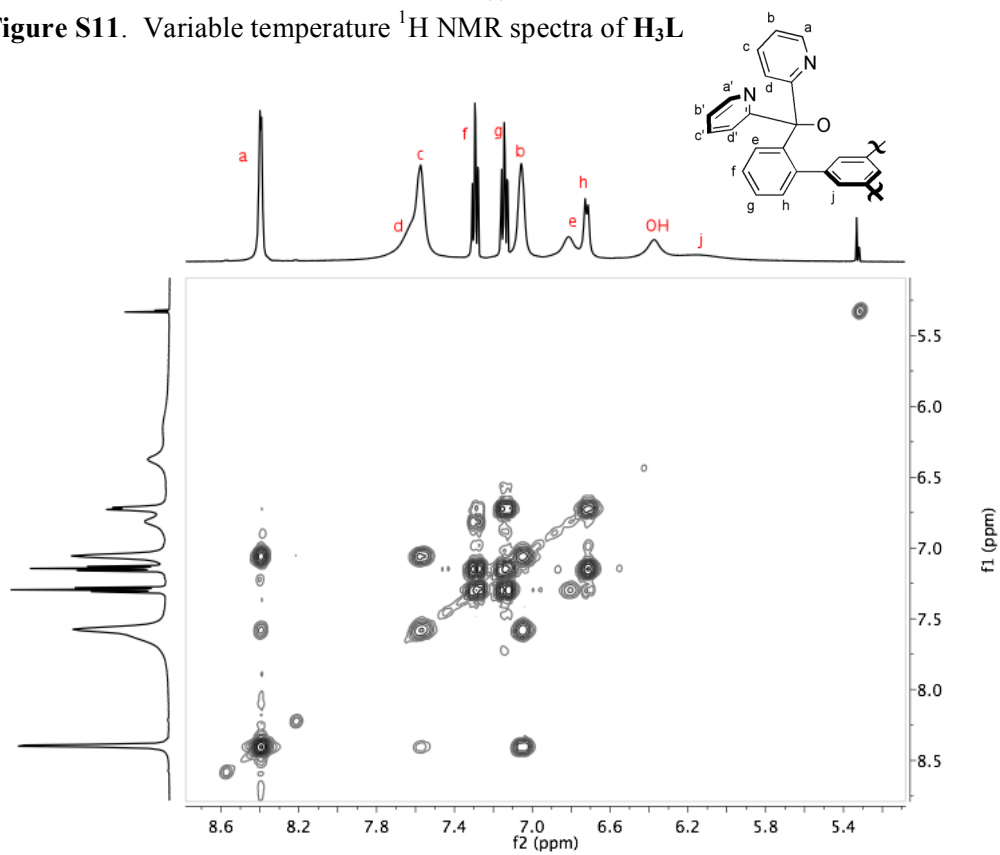


Figure S12. gCOSY NMR spectrum of H_3L in CD_2Cl_2 at $25\text{ }^\circ\text{C}$.

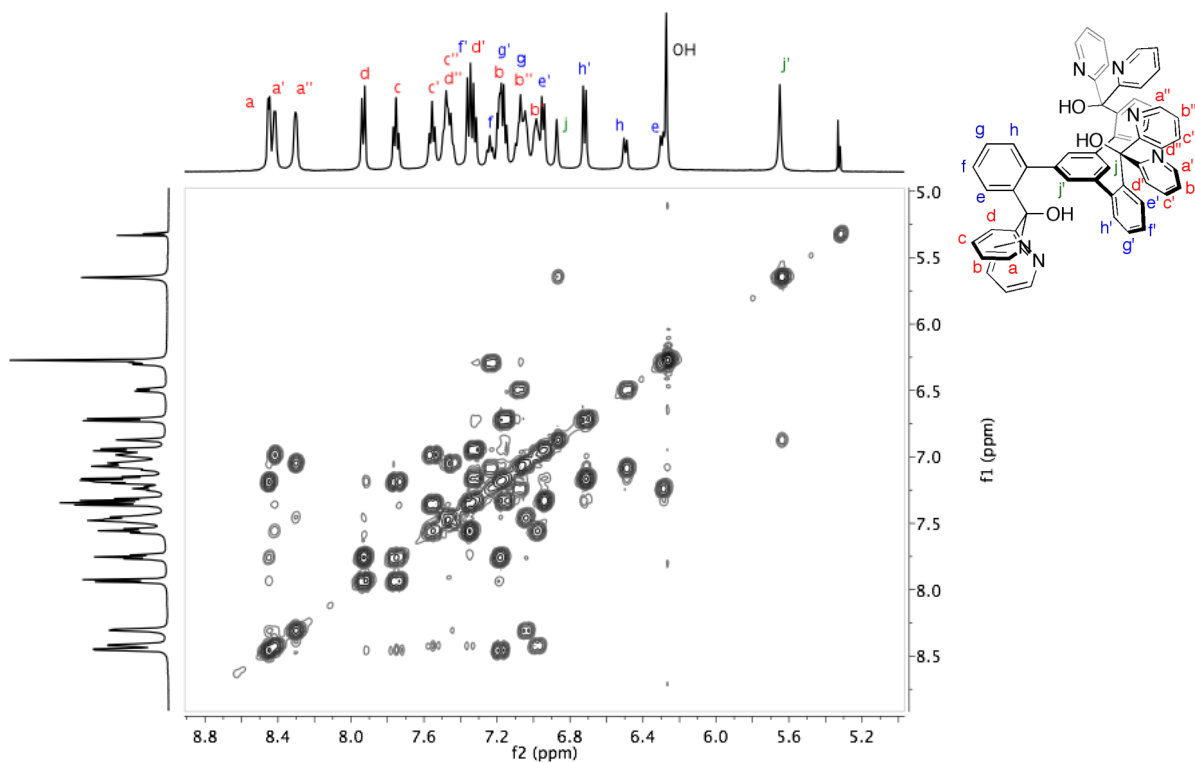


Figure S13. gCOSY NMR spectrum of **H₃L** in CD_2Cl_2 at $-50\text{ }^\circ\text{C}$.

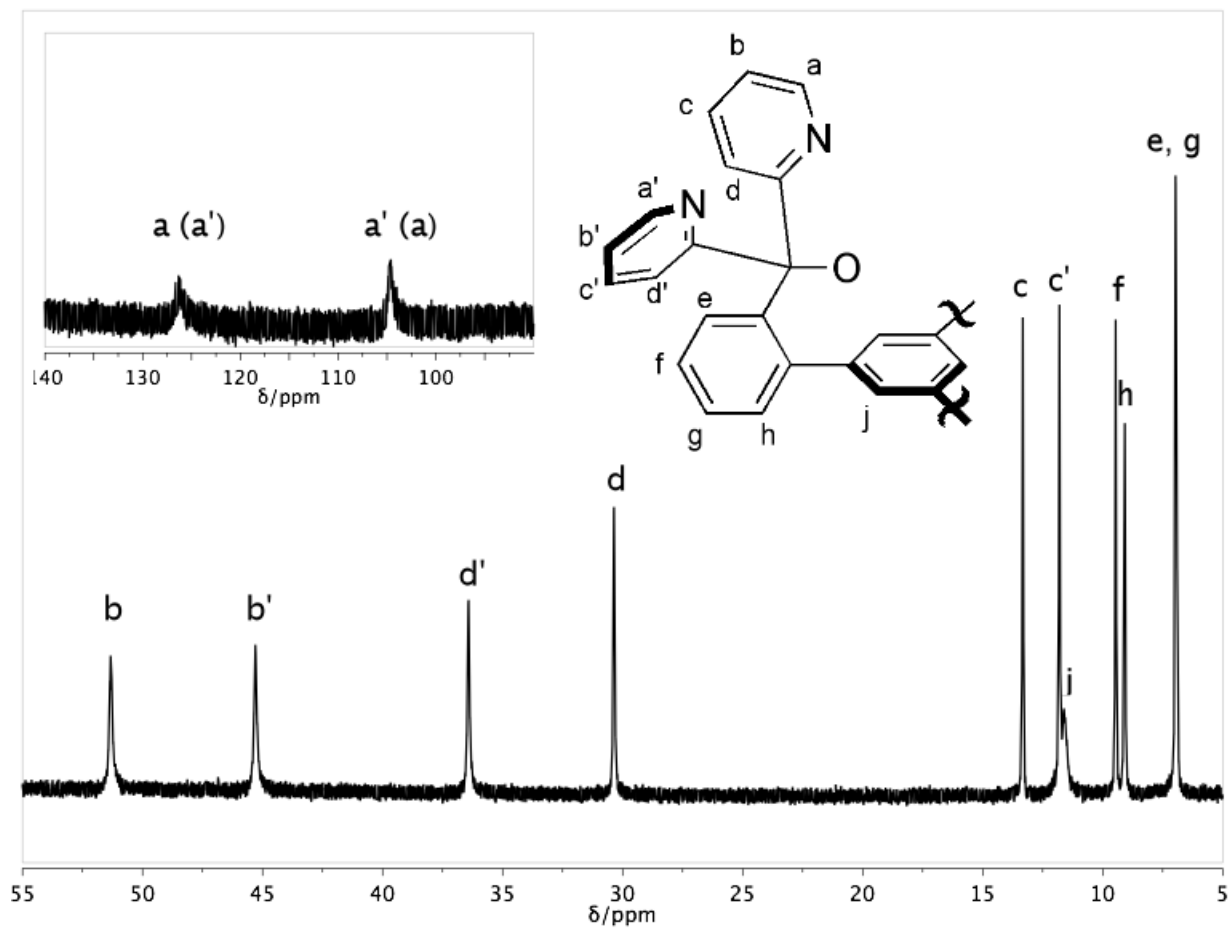


Figure S14. ¹H NMR spectrum of **2•3OTf** in CD₃CN at 25 °C.

Table S1. Signal assignments, shifts, and relaxation times of the ¹H NMR spectrum of **2•3OTf**.

H	δ (ppm)	T ₁ (ms)	T ₂ (ms)
a or a'	126.72	3	1
a or a'	104.99	4	1
b	51.44	27	7
b'	45.43	20	8
d'	36.53	40	11
d	30.42	56	14
c	13.34	91	20
c'	11.81	67	20
j	11.61	8	5
f	9.47	98	20
h	9.08	46	18
g	6.96	105	19
e	6.91	32	19

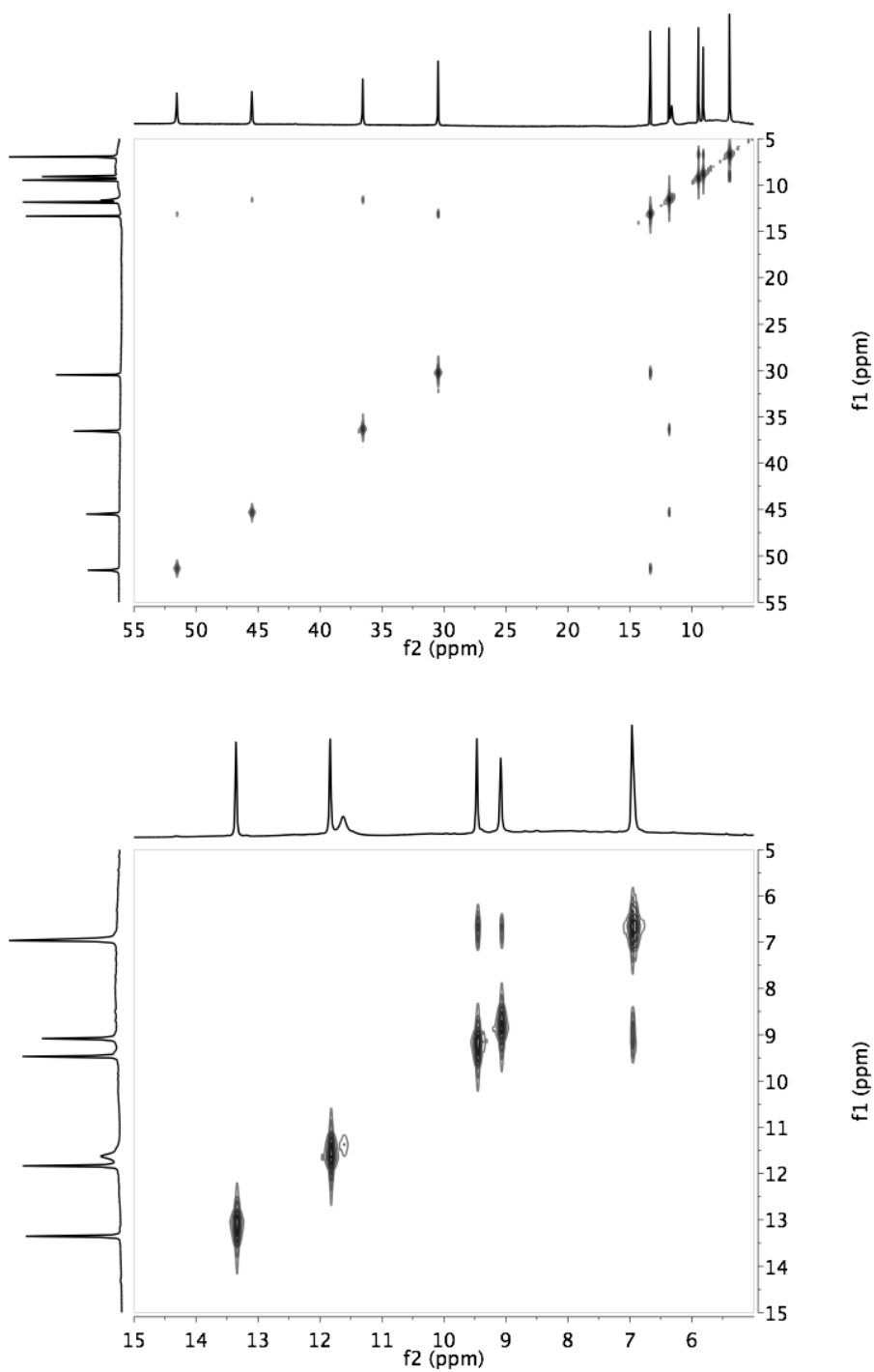


Figure S15. gCOSY NMR spectra of **2•3OTf** in CD_3CN at $25\text{ }^\circ C$.

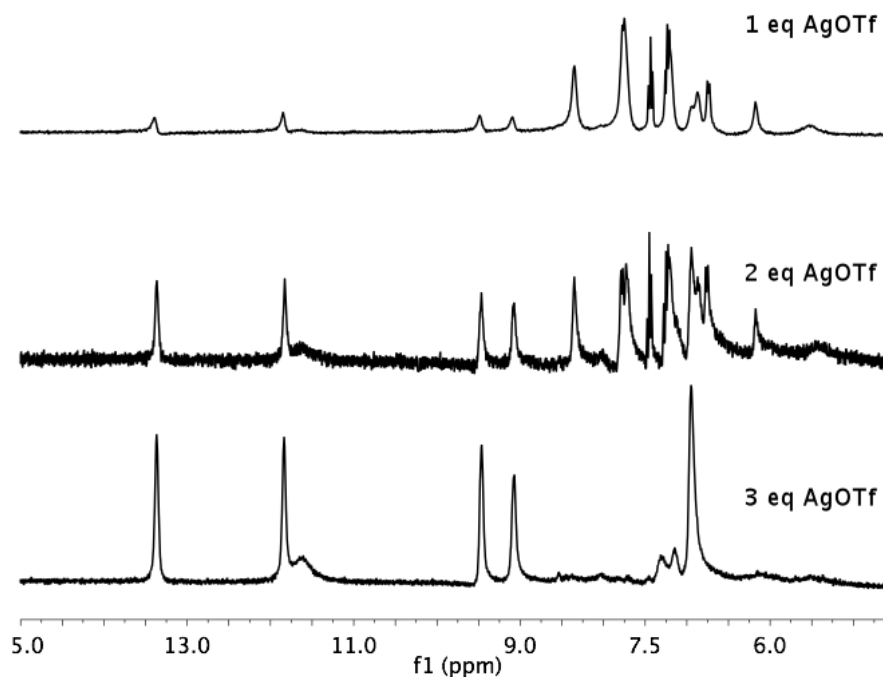


Figure S16. ^1H NMR spectra of the reactions mixtures of the addition of AgOTf and Et_3N to **1•3OTf**.

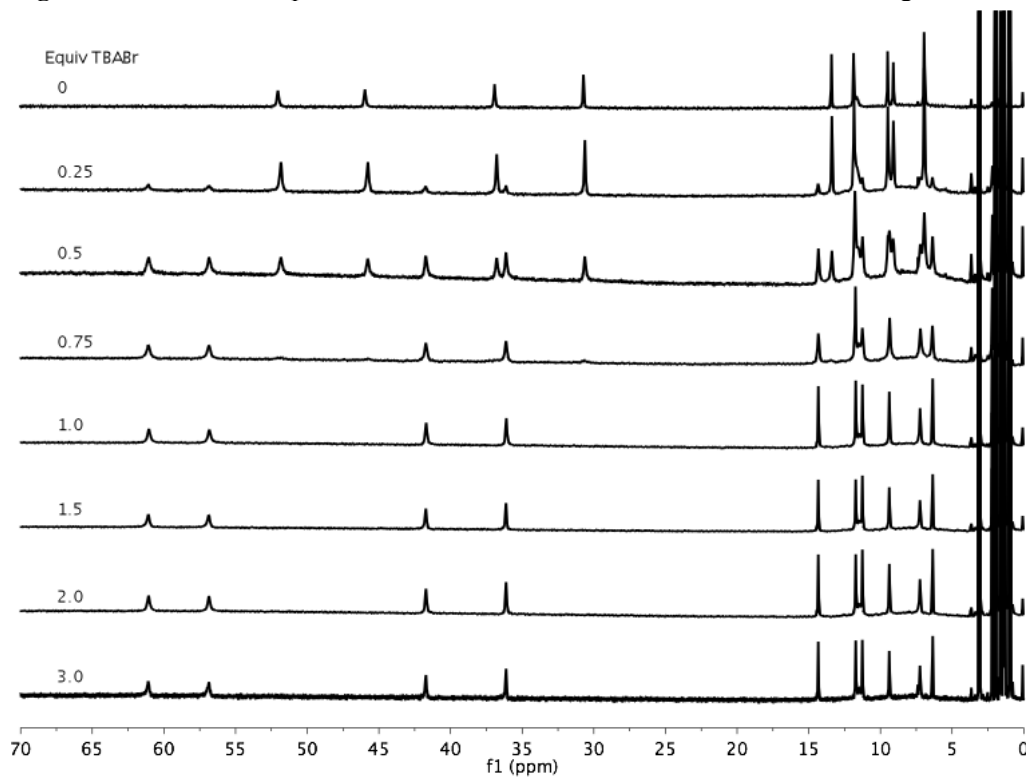


Figure S17. Room temperature ^1H NMR spectra of reactions mixtures upon addition of $n\text{Bu}_4\text{NBr}$ to a CD_3CN solution of **2•3OTf**. Four broad signals downfield of 70 ppm not shown for clarity.

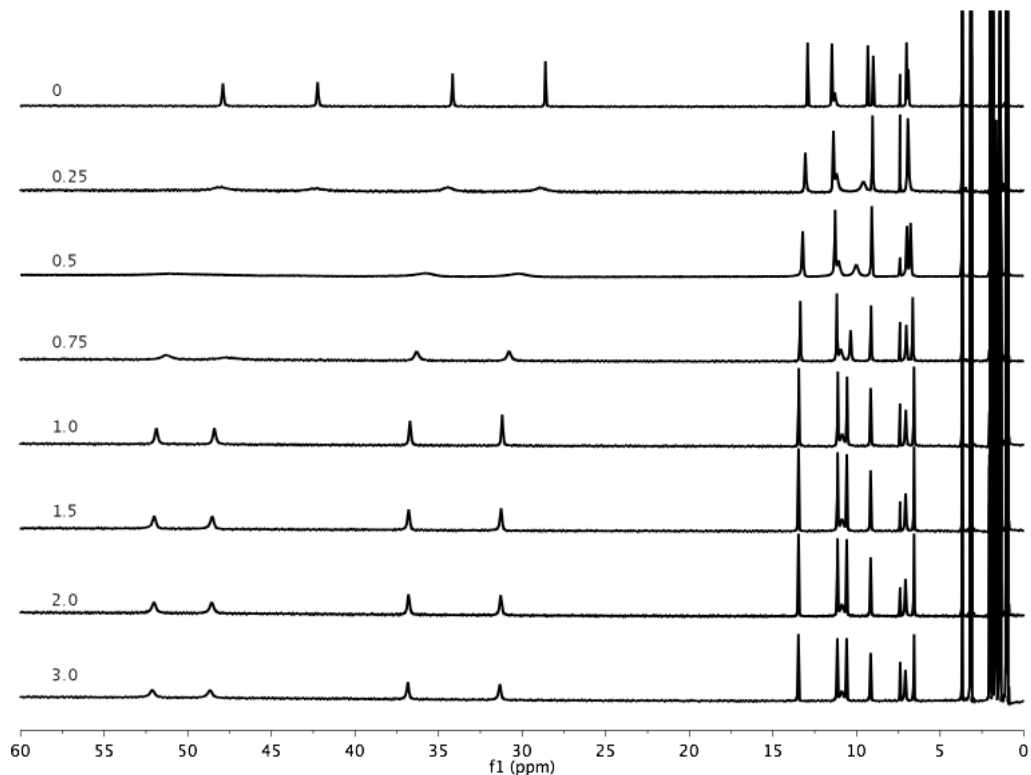


Figure S18. ^1H NMR spectra taken at $65\text{ }^\circ\text{C}$ of reaction mixtures upon addition of $n\text{Bu}_4\text{NI}$ to a CD_3CN solution of $2\cdot 3\text{OTf}$. Two broad signals downfield of 60 ppm not shown for clarity.

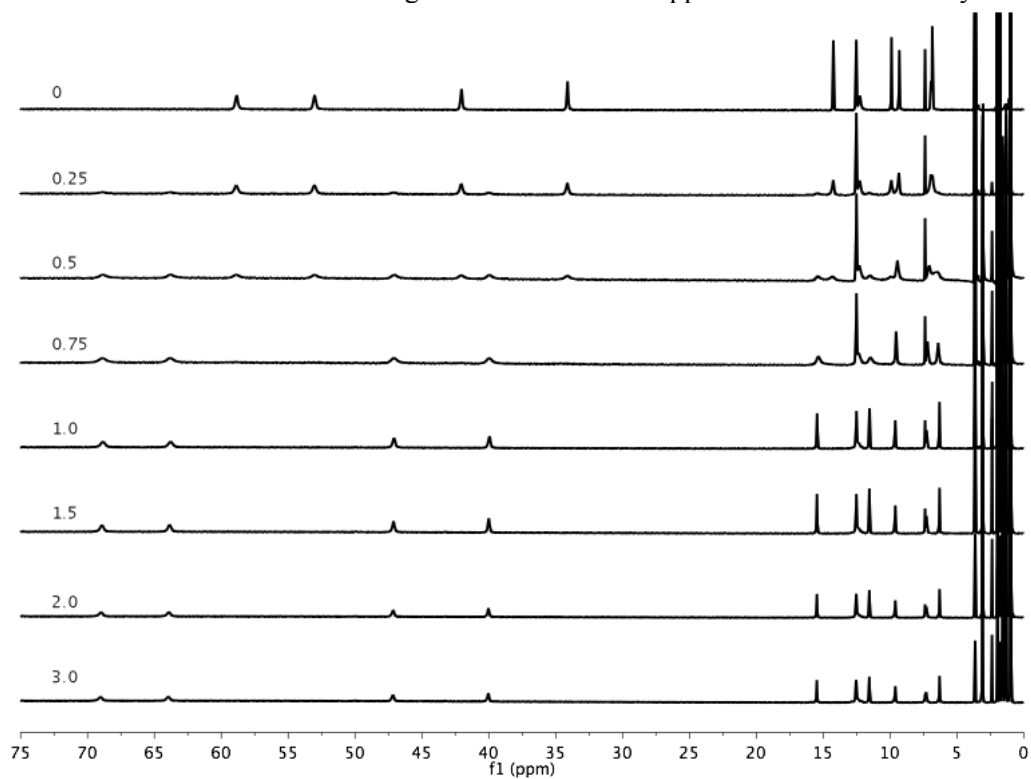


Figure S19. ^1H NMR spectra taken at $-35\text{ }^\circ\text{C}$ of reaction mixtures upon addition of $n\text{Bu}_4\text{NI}$ to a CD_3CN solution of $2\cdot 3\text{OTf}$. Four broad signals downfield of 75 ppm not shown for clarity.

Magnetic Susceptibility Measurements

General Considerations. The magnetic susceptibility measurements were carried out in the Molecular Materials Research Center in the Beckman Institute of the California Institute of Technology on a Quantum Design MPMS instrument running MPMS Multivu software. Crystalline samples (0.030–0.100 g) were powdered and suspended in a clear plastic straw in gel caps. Data were recorded at 0.5 and 5 T from 4–300 K. Diamagnetic corrections were made using the average experimental magnetic susceptibility of $\mathbf{H}_3\mathbf{L}$ at 0.5 T from 100–300 K ($-593 \times 10^{-6} \text{ cm}^3/\text{mol}$) in addition to the values of Pascal's constants for amounts of anion and solvent quantified for each sample using elemental analysis.

The $\chi_M T$ data taken at 0.5 T were initially fit to the magnetic susceptibility equation derived from the isotropic spin Hamiltonian for two coupling constants, J and J_{13} [Eq. (1)]. The best fit was found with $\alpha = J_{13}/J = 1$, so the data were instead modeled to an equilateral triangle of $S = 1/2$ spins [Eq. (2, 3)].

$$\hat{H} = -2J[(\hat{S}_1\hat{S}_2) + (\hat{S}_2\hat{S}_3)] - 2J_{13}(\hat{S}_3\hat{S}_1) \quad (1)$$

$$\hat{H} = -2J[(\hat{S}_1\hat{S}_2) + (\hat{S}_2\hat{S}_3) - (\hat{S}_3\hat{S}_1)] \quad (2)$$

$$\chi_M = \frac{Ng^2\beta^2}{4k(T-\theta)} \left[\frac{5 + \exp(-3J/kT)}{1 + \exp(-3J/kT)} \right] \quad (3)$$

The data were fit using Matlab^[4] (contact author for code) by minimizing

$R = \sum |(\chi_M T)_{obs} - (\chi_M T)_{calcd}|^2 / \sum (\chi_M T)_{obs}^2$ (Table S2). The data for $\mathbf{2}\cdot\mathbf{3BF}_4\cdot\mathbf{Et}_2\mathbf{O}$ could not be satisfactorily fit without the inclusion of a temperature independent magnetism $-500 \times 10^{-6} \text{ cm}^3/\text{mol}$, which may be attributed to the presence of diamagnetic impurities such as unaccounted for solvent in the material.

The magnetic parameters when the data are fit with an additional Curie-Weiss parameter θ are shown in Table S2, Figure S20, and Figure S21. The variables were modeled from multiple starting values, and the fitted parameters were stable within reasonable ranges for J (-60 to 0 cm^{-1}), g (1.90 to 2.10), and θ (-2 to 2 K), except for compound $\mathbf{2}\cdot\mathbf{PO}_4$, whose fit showed a second local minimum with values of $J = 1.0 \text{ cm}^{-1}$, $g = 2.10$, and $\theta = -4.5 \text{ K}$. This set of parameters was not favored because of its large θ value and because the R value was slightly higher (0.9×10^{-4}).

The parameters fit without θ are shown in Table S3, Figure S22, and Figure S23.

Table S2. Magnetic parameters with included θ .

Compound	Diamagnetic Correction ($\times 10^{-6} \text{ cm}^3/\text{mol}$)	$J (\text{cm}^{-1})$	g	$\theta (\text{K})$	$R (\times 10^{-4})$
$\mathbf{2}\cdot\mathbf{PO}_4\cdot\mathbf{H}_3\mathbf{PO}_4\cdot\mathbf{6H}_2\mathbf{O}$	-782	-2.7	2.09	1.7	0.7
$\mathbf{2}\cdot\mathbf{3OTf}$	-881	-52	2.10	-0.6	0.3
$\mathbf{2}\cdot\mathbf{3BF}_4\cdot\mathbf{Et}_2\mathbf{O}$	-737	-52.2	2.10	-1.6	4.2
$\mathbf{3}\cdot\mathbf{Br}\cdot\mathbf{2OTf}\cdot\mathbf{THF}$	-837	-7.3	1.98	0.8	2.3
$\mathbf{3}\cdot\mathbf{I}\cdot\mathbf{2OTf}$	-803	-22.0	1.95	1.0	5.7

Table S3. Parameters when fit without θ .

Compound	$J (\text{cm}^{-1})$	g	$R (\times 10^{-4})$
$\mathbf{2}\cdot\mathbf{PO}_4\cdot\mathbf{H}_3\mathbf{PO}_4\cdot\mathbf{6H}_2\mathbf{O}$	-1.3	2.08	4.5
$\mathbf{2}\cdot\mathbf{3OTf}$	-49.1	2.07	1.6
$\mathbf{2}\cdot\mathbf{3BF}_4\cdot\mathbf{Et}_2\mathbf{O}$	-51.3	1.96	13
$\mathbf{3}\cdot\mathbf{Br}\cdot\mathbf{2OTf}\cdot\mathbf{THF}$	-6.5	1.98	7.6
$\mathbf{3}\cdot\mathbf{I}\cdot\mathbf{2OTf}$	-22.7	1.97	12

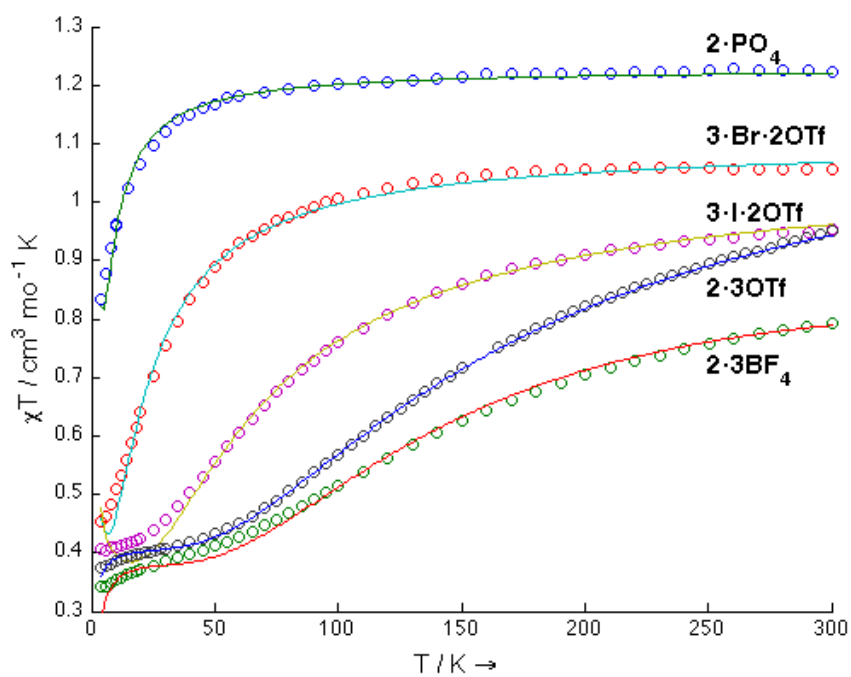


Figure S20. $\chi_M T$ vs. T plots with fits for compounds **2** and **3** using parameters from Table S2.

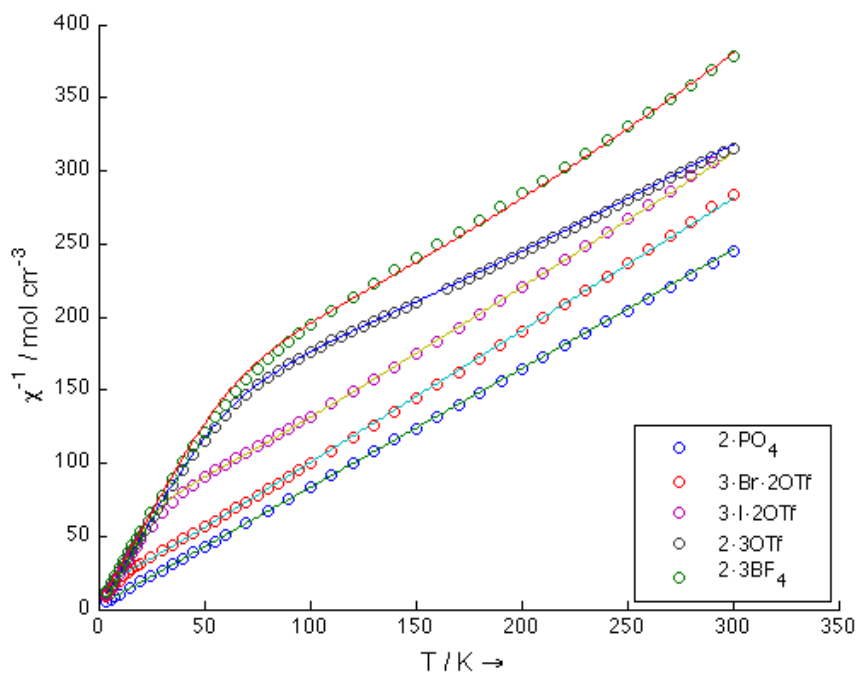


Figure S21. χ_M^{-1} vs. T plots with fits for compounds **2** and **3** using parameters from Table S2.

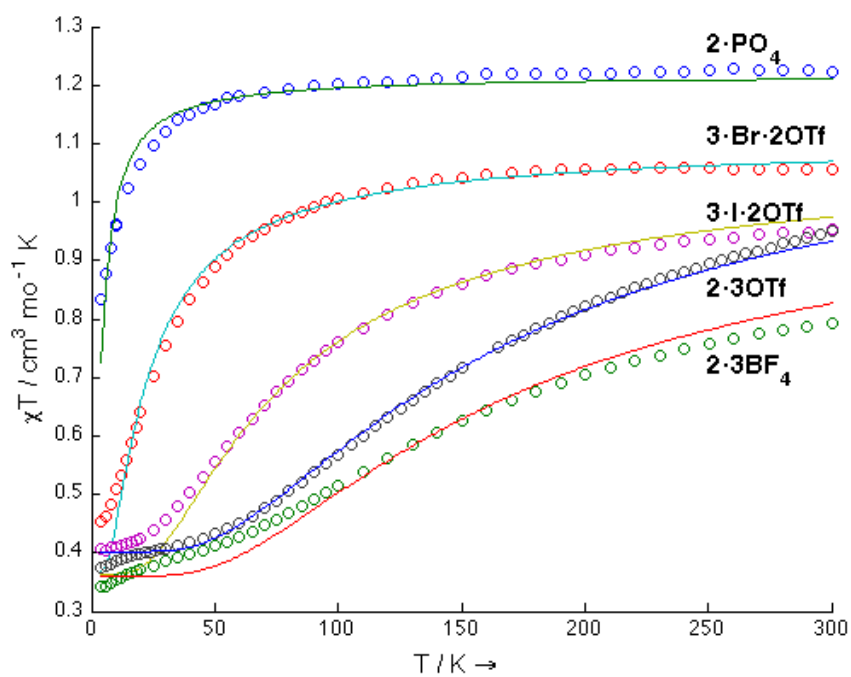


Figure S22. $\chi_M T$ vs. T plots with fits for compounds **2** and **3** using parameters from Table S3.

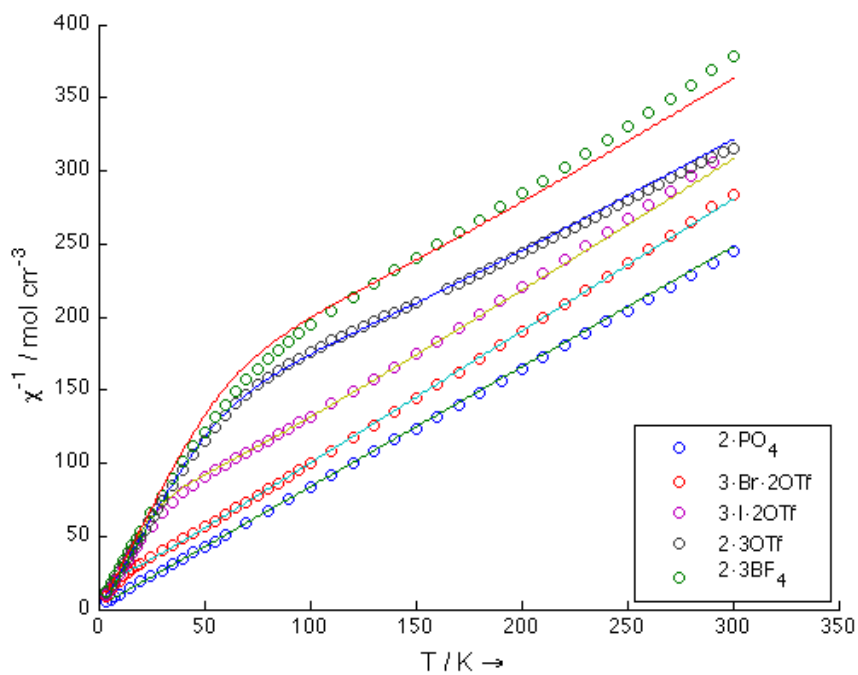
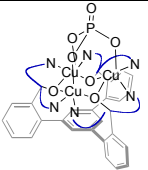
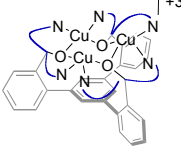
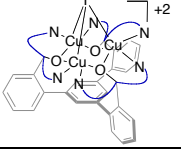
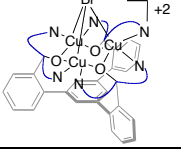
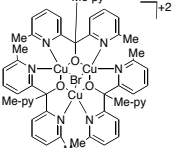
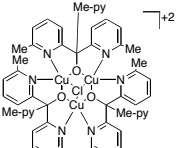
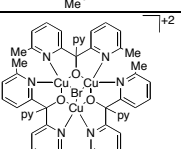
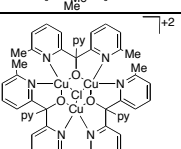
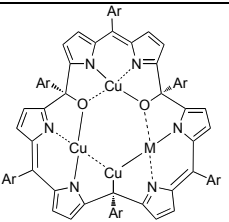
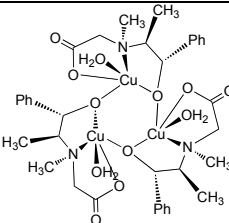
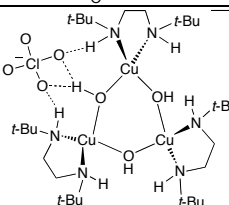


Figure S23. χ_M^{-1} vs. T plots with fits for compounds **2** and **3** using parameters from Table S3.

Magnetostructural Study

Table S4. Structural and magnetic parameters for alkoxo- or hydroxo-bridged copper(II) trimers in this work and in the literature.

Compound	Structure	Cu–O–Cu Angle (°)	J (cm ⁻¹)
2•PO₄		114.6–118.5	-2.7
2•3OTf		125.9–126.5	-52.0
3•1•2OTf		116.7–120.8	-22.0
3•Br•2OTf		116.1–118.5	-7.3
a1^[5]		116.4	-19.5
a2^[5]		114.5	-3.7
a3^[5]		114.4	-4.8
a4^[5]		114.0	-0.3

b ^[6]		121.2–125.2	-44
c ^[7]		131.1	-57
d ^[8]		144.3	-104.7

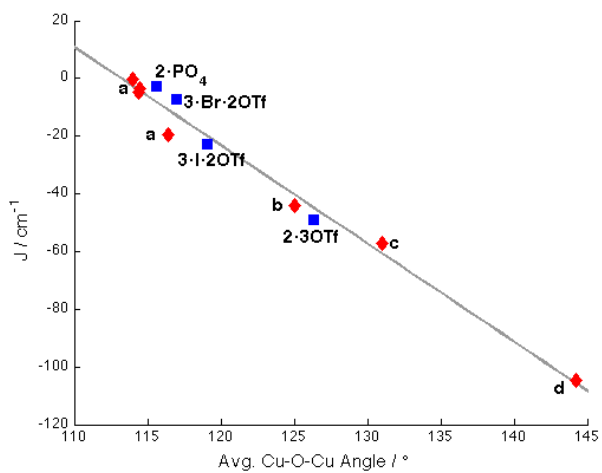


Figure S24. Plot of J vs. bridge angle for the series of alkoxy- or hydroxo-bridged copper(II) trimers presented in Table S4.

EPR Measurements

X-band EPR spectra were obtained on a Bruker EMX Biospin spectrometer. Variable temperature measurements were conducted with an Oxford continuous-flow helium cryostat. EPR parameters were simulated using W95EPR.^[5]

The complexes were studied using X-band EPR spectroscopy in solution and in the solid state. The EPR spectrum of **2•3OTf** in ethanol solution at 10 K (Figure S24) shows a feature at around $g = 2$ arising from the doublet ground state. The EPR spectra of **2•3BF₄**, **3•I•2OTf**, and **3•Br•2OTf** are similar, with varying amounts of broadness (Figure S27). However, the EPR spectrum of **2•PO₄** shows an additional broad feature at around 1700 G. The low-field signal is characteristic of a $S = 3/2$ excited state.^[6] As the temperature increases, the intensity of the low-field signal increases relative to that of the higher-field feature, suggesting a spin equilibrium between the quartet and doublet spin states, with the doublet state as the ground state in agreement with the small antiferromagnetic exchange interaction determined from the magnetic susceptibility data (Figure S25). The variation in EPR spectra between **2•3OTf** and **2•PO₄** is explained by the antiferromagnetic exchange between copper centers. Since $J = -2.7 \text{ cm}^{-1}$ in **2•PO₄**, the $S = 3/2$ state is thermally populated even at 10 K and EPR transitions within this quartet state can be observed. In contrast, at the same temperatures no low field EPR signals are observed in the other copper(II) complexes due to the larger antiferromagnetic exchange and doublet-quartet state energy splittings.

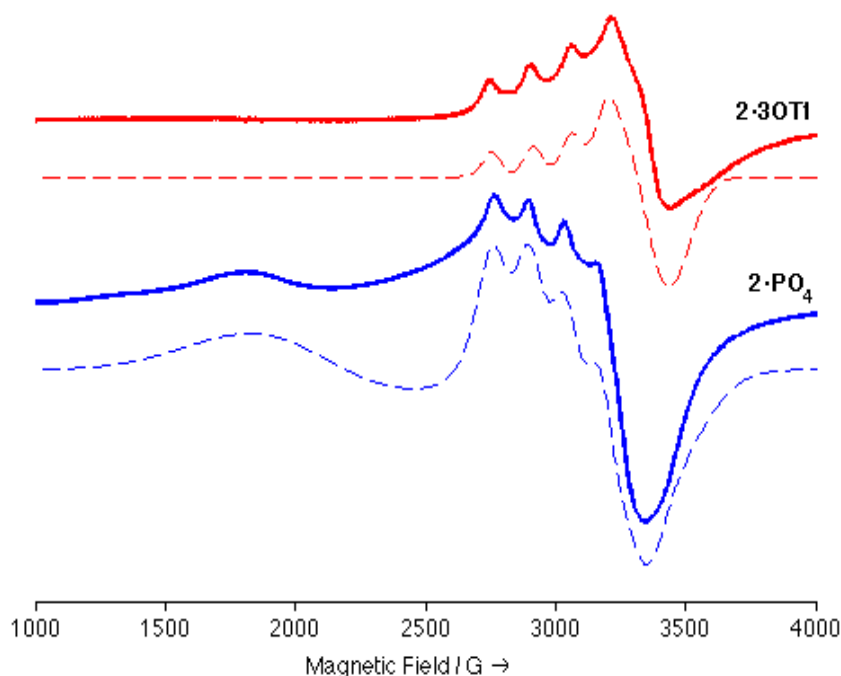


Figure S25. Experimental (—) and simulated (- -) X-band EPR spectra of **2•3OTf** and **2•PO₄** in ethanol solution at 10 K. Simulated parameters: **2•3OTf**: $g_{\perp} = 1.98$, $g_{\parallel} = 2.24$, and $A_{\parallel} = 0.015 \text{ cm}^{-1}$. **2•PO₄** was simulated as two systems: a) $g_{\perp} = 2.08$, $g_{\parallel} = 2.24$, $A_{\perp} = 0.011 \text{ cm}^{-1}$, $A_{\parallel} = 0.014 \text{ cm}^{-1}$ and b) $g_{\perp} = 3.40$, $g_{\parallel} = 2.00$, $A_{\perp} = 0.007 \text{ cm}^{-1}$, and $A_{\parallel} = 0.001 \text{ cm}^{-1}$.

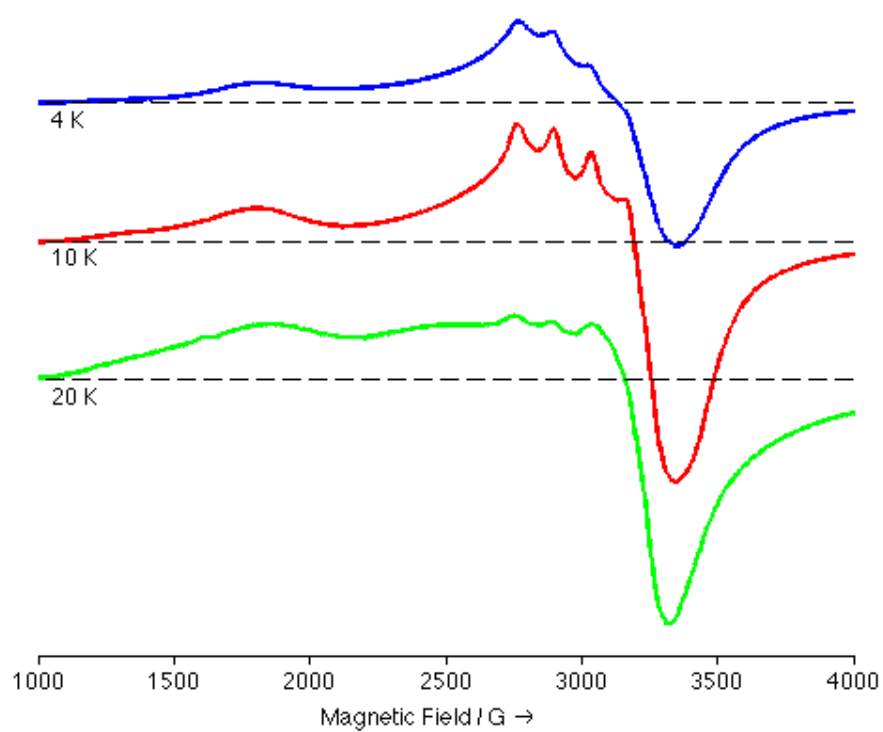


Figure S26. EPR spectra of $2\bullet\text{PO}_4$ in ethanol solution at 4, 10, and 20 K.

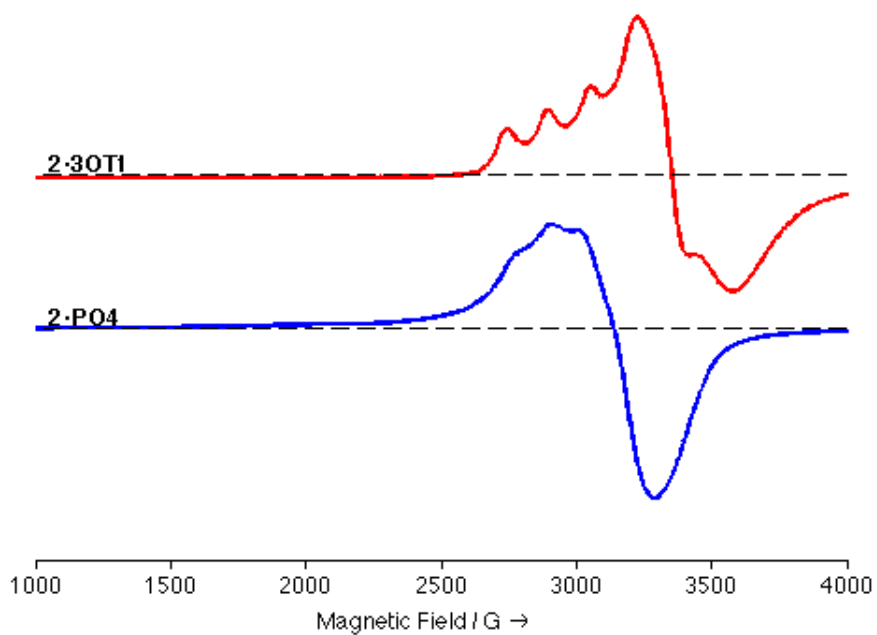


Figure S27. Powder X-band EPR spectra of $2\bullet 3\text{OTf}$ and $2\bullet\text{PO}_4$ at 10 K.

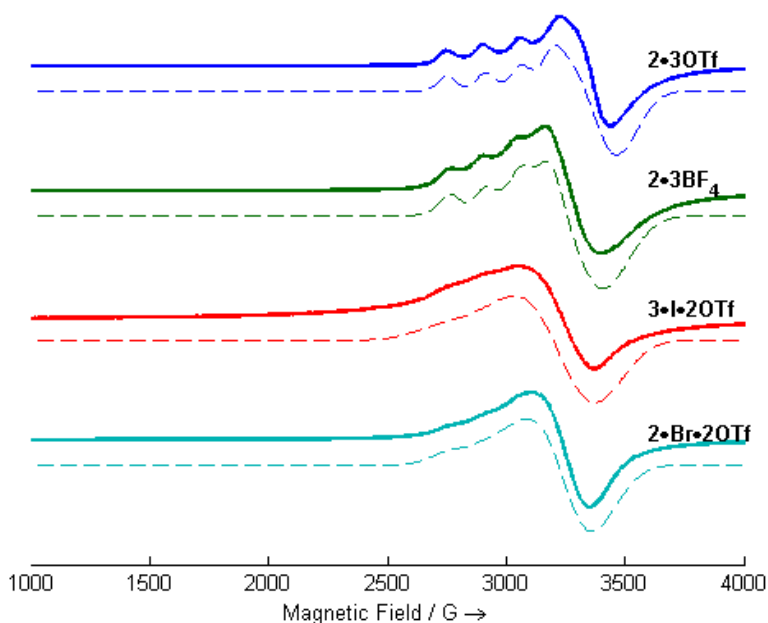


Figure S28. Experimental (–) and simulated (–) EPR spectra of CH_3CN solutions of **2•3OTf**, **2•3BF₄**, **3•I•2OTf**, **3•Br•2OTf** at 10 K. Simulated parameters: **2•3OTf**: $g_{\perp} = 1.97$, $g_{\parallel} = 2.24$, $A_{\perp} = 0 \text{ cm}^{-1}$, $A_{\parallel} = 0.015 \text{ cm}^{-1}$. **2•3BF₄**: $g_{\perp} = 2.01$, $g_{\parallel} = 2.23$, $A_{\perp} = 0.001 \text{ cm}^{-1}$, $A_{\parallel} = 0.014 \text{ cm}^{-1}$. **3•I•2OTf**: $g_{\perp} = 2.04$, $g_{\parallel} = 2.29$, $A_{\perp} = 0.007 \text{ cm}^{-1}$, $A_{\parallel} = 0.015 \text{ cm}^{-1}$. **3•Br•2OTf**: $g_{\perp} = 2.05$, $g_{\parallel} = 2.25$, $A_{\perp} = 0 \text{ cm}^{-1}$, $A_{\parallel} = 0.015 \text{ cm}^{-1}$. Parameters for **3•I•2OTf** and **3•Br•2OTf** are approximate due to the broadness of the signals.

References

- (1) K. M. Gillespie, C. J. Sanders, P. O'Shaughnessy, I. Westmoreland, C. P. Thickitt, P. Scott, *J. Org. Chem.* **2002**, *67*, 3450.
- (2) H.-C. Liang, K. D. Karlin, R. Dyson, S. Kaderli, B. Jung, A. D. Zuberbühler, *Inorg. Chem.* **2000**, *39*, 5884.
- (3) X. L. Feng, J. S. Wu, V. Enkelmann, K. Mullen, *Org. Lett.* **2006**, *8*, 1145.
- (4) *Matlab*, version 7.6.0 (R2008a); The MathWorks, Inc.: Natick, MA 2008.
- (5) M. Kodera, Y. Tachi, T. Kita, H. Kobushi, Y. Sumi, K. Kano, M. Shiro, M. Koikawa, T. Tokii, M. Ohba, H. Okawa, *Inorg. Chem.* **2000**, *39*, 226.
- (6) M. Inoue, C. Ikeda, Y. Kawata, S. Venkatraman, K. Furukawa, A. Osuka, *Angew. Chem.* **2007**, *119*, 2356; *Angew. Chem. Int. Ed.* **2007**, *46*, 2306.
- (7) H. Lopez-Sandoval, R. Contreras, A. Escuer, R. Vicente, S. Bernes, H. Noth, G. J. Leigh, N. Barba-Behrens, *J. Chem. Soc. Dalton Trans.* **2002**, 2648.
- (8) L. M. Mirica, T. D. P. Stack, *Inorg. Chem.* **2005**, *44*, 2131.
- (9) F. Neese, *QCPE Bull.* **1995**, *15*, 5.
- (10) a) P. Fleischhauer, S. Gehring, C. Saal, W. Haase, Z. Tomkowicz, C. Zanchini, D. Gatteschi, D. Davidov, A. L. Barra, *J. Magn. Magn. Mater.* **1996**, *159*, 166; b) I. A. Koval, H. Akhidenov, S. Tanase, C. Belle, C. Duboc, E. Saint-Aman, P. Gamez, D. M. Tooke, A. L. Spek, J.-L. Pierre, J. Reedijk, *New J. Chem.* **2007**, *31*, 512; c) L. Gutierrez, G. Alzuet, J. A. Real, J. Cano, J. Borrás, A. Castineiras, *Inorg. Chem.* **2000**, *39*, 3608; d) L. Banci, A. Bencini, D. Gatteschi, *Inorg. Chem.* **1983**, *22*, 2681.